

**Universidade do Minho**
Escola de Engenharia

Rita Francisco dos Santos

# Optimization of microfluidic chip procedures for point-of-care blood-plasma extraction

july 2025

Optimization of microfluidic chip procedures for point-of-care blood-plasma extraction

Rita Francisco dos Santos

UMinho | 2025

**University of Minho**
School of Engineering

Rita Francisco dos Santos

# Optimization of microfluidic chip procedures for point-of-care blood-plasma extraction

Master's Dissertation
Master's in Biomedical Engineering
Medical Electronics Branch

Work carried out under the supervision of
**Dr. Vanessa Cardoso, University of Minho**

**Dr. Inês Mendes Pinto, Institute for Research and Innovation in Health, University of Porto**

july 2025

# COPYRIGHTS AND CONDITIONS OF USE OF THIS WORK BY THIRD PARTIES

This is an academic work that can be used by third parties as long as the internationally accepted rules and good practices are respected, with regard to copyrights and related rights.

Thus, the present work can be used under the terms foreseen by the license indicated below.

If the user needs permission to be able to use the work under conditions not provided for in the indicated licensing, he/she should contact the author, through the RepositóriUM of the University of Minho.

***License conceded to the users of this work:***



**Atribuição-NãoComercial-SemDerivações**
**CC BY-NC-ND**

https://creativecommons.org/licenses/by-nc-nd/4.0/

# ACKNOWLEDGEMENTS

A finalização deste mestrado é mais do que concluir uma etapa académica; é a realização de um desafio que exigiu muita dedicação, resiliência e crescimento, num dos anos mais difíceis da minha vida a nível pessoal.

Assim, gostaria de começar por expressar a minha profunda gratidão às minhas orientadoras, Drª Vanessa Cardoso e Drª Inês Mendes Pinto, por toda a disponibilidade, paciência, compreensão, e apoio incondicional. Obrigada por acreditarem em mim enquanto aluna e por tornarem este percurso, apesar de atribulado, o mais tranquilo possível. O vosso incentivo, as palavras de encorajamento e o carinho que me transmitiram ao longo desta jornada foram fundamentais. Enfrentei muitos desafios, com altos e baixos, mas tive a sorte de ter as melhores orientadoras ao meu lado.

Quero igualmente agradecer do fundo do coração aos meus pais, pelo amor incondicional, paciência e força que sempre me deram. Obrigada por lutarem por mim e por estarem sempre disponíveis 24/7. Sem vocês, nada disto seria possível. Serão um exemplo de amor, coragem e resiliência para todo o sempre. Ao meu gatinho gordinho, Kiko, obrigada por cresceres comigo nos últimos 14 anos, foi um prazer. Quando era mais nova disse que quando terminasse o curso iria tirar uma foto contigo, mas tal não será possível. O teu abracinho ficará para sempre na minha memória.

À minha melhor amiga, Guida, obrigada por mais de uma década de amizade e por me apoiares incondicionalmente ao longo de todos estes anos. Que possamos continuar assim, até sermos velhinhas. Quero agradecer também à Marta, pela amizade que me acompanhou desde o primeiro ao último ano da universidade. Foi um privilégio realizar este percurso contigo. Ao Rúben, obrigada por me "aturares" e por me deixares ser a tua "vela favorita" nestes últimos anos. A tua personalidade divertida tornou tudo mais leve. Quero agradecer também ao Xico e à Rora. Ao Xico, pela amizade inestimável, pelos momentos inesquecíveis e por todos estes anos em que crescemos juntos. À Rora, por ser uma amiga incrível, cheia de loucura e de alegria. A todos vocês, obrigada pelas risadas, pelas longas conversas no "Cachorrão" e na casa da Guida. Este ano, a vossa companhia foi ainda mais especial e importante para mim.

Ao Zé, o meu bestie, obrigada por teres aparecido na minha vida. Foi uma surpresa boa. A tua paciência e amizade foram fundamentais ao longo dos últimos dois anos, especialmente neste último, que teria sido ainda mais difícil sem ti. Agora, um agradecimento especial ao meu grupo mais recente, os "NACI'S.". À Carol, obrigada pelas palavras sempre carinhosas e pela tua amizade incondicional! Ao

Gabriel, obrigada por tornares as minhas últimas memórias de 2024 ainda mais especiais e por me "aturares" nesses últimos meses. Ao Sérgio, agradeço as palavras de apoio que significaram tanto. Ao Rex polícia e ao Vitor, obrigada pela vossa personalidade única e pelo humor contagiante que me arrancou tantas gargalhadas. À Bea, Pipa, Andreia, Sara, Lídia e Afonso, não poderia deixar de agradecer todas as conversas, piadas e momentos que me fizeram rir ao longo dos últimos meses de 2024 e 2025. A todos os "NACI's", obrigada pelas boleias, pelas saídas e por todos os restantes momentos. Por mais cansada que esteja, a vossa presença fez-me sempre feliz. Direta ou indiretamente, vocês foram das pessoas mais importantes do meu último ano, e a vossa companhia foi sem dúvida essencial para mim.

Ao "Peste", obrigada pelos últimos 5 anos, repletos de momento felizes. Sei que este ano não fui tão presente quanto gostaria, mas a vida continua e é um prazer e orgulho ver cada um de nós tornar-se engenheiro. Um agradecimento especial à Banshee e à Mo, pela amizade que levarei comigo para sempre. E claro à minha parceira de mestrado, a Apita, o que seria de mim sem ti neste ano difícil. Obrigada por ouvires todos os meus desabafos, e por estares sempre ao meu lado. Quero também expressar a minha gratidão às minhas "roomies", Ju e Vaivém, por tudo. Em especial à Vaivém, pelas palavras de conforto que me disse em momentos menos bons. Ao meu padrinho, Gummy, agradeço todas as palavras e abraços que me deu ao longo do meu percurso académico. A tua presença foi essencial, e serei sempre grata pelo apoio incondicional que me deste.

Ao *IEEE UMinho Student Branch*, obrigada por todas as memórias e aprendizagens que levarei comigo para a vida. Foram também uma ajuda enorme neste caminho difícil. Um agradecimento especial às minhas meninas e meninos, Andreia, Bia, Gabi, Manu, Andrés, Simão, Leote e Socker.

Agradeço igualmente a todas as pessoas que me acompanharam ao longo da vida, pois, mesmo que não estejam mencionadas aqui, tiveram um papel importante nesta caminhada. Família, amigos e professores: levarei um bocado de cada um comigo para sempre.

"*Last but not least I want to thank me...I wanna thank me for believing in me, I want to thank me for doing all this hard work. (...) I wanna thank me for never quitting. (...) I wanna thank me for just being me at all times*"- *Snoop Dogg*.

# STATEMENT OF INTEGRITY

I hereby declare having conducted this academic work with integrity. I confirm that I have not used plagiarism or any form of undue use of information or falsification of results along the process leading to its elaboration.

I further declare that I have fully acknowledged the Code of Ethical Conduct of the University of Minho (UMinho) and the Institute for Research and Innovation in Health (i3S), University of Port

# RESUMO

O sangue é o fluido corporal mais estudado para fins de diagnóstico. A sua análise fornece informações essenciais sobre vários parâmetros fisiológicos, sendo por isso, uma ferramenta indispensável tanto no diagnóstico como na monitorização de doenças.

No entanto, os métodos convencionais de recolha e análise de sangue requerem volumes de amostra significativos (~7.5mL), envolvem procedimentos invasivos e necessitam de um pré-processamento laboratorial extenso. Além disso, estes métodos são morosos, e dependem de equipamentos complexos, o que os tornam inadequados para o diagnóstico e monitorização de rotina no âmbito dos cuidados de saúde primários. Neste contexto, a capacidade de realizar testes de diagnóstico no local de prestação de cuidados (*point-of-care*, PoC) é crucial para assegurar intervenções clínicas atempadas, promovendo a eficácia terapêutica e a melhoria dos cuidados de saúde.

Para fazer face a estas limitações, as tecnologias microfluídicas oferecem uma alternativa promissora, permitindo o processamento minimamente invasivo de amostras de sangue (por exemplo, uma gota de sangue capilar) em dispositivos compactos e miniaturizados. Em particular, os sistemas microfluídicos podem facilitar a extração de plasma de sangue total na gama dos microlitros, eliminando a necessidade de um pré-processamento externo e extensivo.

Assim, esta dissertação tem como objetivo otimizar o processo de utilização de um chip microfluídico, de forma a permitir e maximizar a extração de plasma de uma pequena amostra de sangue capilar obtida através de uma punção no dedo. Este chip é composto por uma interface *Luer* para a entrada da amostra sanguínea, um canal de suporte, uma membrana de filtração com 10 mm de diâmetro, um canal de recolha de plasma, um canal de ventilação e interfaces para aplicação de vácuo e alívio de pressão. Além do chip, são utilizados acessórios complementares como um reservatório para a introdução da amostra, e um tampão com conexão *mini Luer*, para o controlo adequado das interfaces. De forma a atingir o objetivo proposto, são realizados ensaios para avaliar parâmetros críticos, incluindo a capilaridade do chip, a força mecânica aplicada aos componentes complementares, bem como o teste de diferentes níveis de diluições da amostra de sangue capilar (não diluído, 1:2 e 1:4), de modo a determinar a abordagem mais eficaz. Assim sendo, a força mecânica consiste na abertura da terceira interface, acompanhada com a aplicação de vácuo na segunda interface, com recurso a uma seringa. A pipeta também é utilizada com o mesmo propósito. A pressão manual através do polegar na tampa do reservatório ou a reinserção e remoção do male mini Luer plug na tampa do mesmo também são

exemplos da força mecânica aplicada ao sistema. Após múltiplos ensaios, os resultados indicam que a abordagem mais eficaz para obter plasma consiste na diluição do sangue total em 1:4, combinada com uma das formas de aplicação de pressão manual sobre o reservatório, referidas anteriormente.

Ao permitir uma colheita minimamente invasiva e um rápido processamento, evitando hemólise e a obstrução da membrana, este sistema microfluídico miniaturizado representa um avanço significativo no desenvolvimento de uma plataforma de diagnóstico integrada e completa. No futuro, esta tecnologia poderá permitir a realização de testes PoC rápidos, económicos e acessíveis, através do processamento, análise e quantificação simultânea e *in situ* de biomarcadores moleculares relacionados, a título de exemplo, com a saúde materno-fetal, permitindo a monitorização da saúde da mãe e do bebé de forma mais rápida e económica no local de prestação de cuidados.

**Palavras-chave:** Chip Microfluídico, Extração Sangue-Plasma, Cuidados de Saúde Primários, Diagnóstico

# ABSTRACT

Blood is the most extensively studied body fluid for diagnostic purposes. Its analysis provides important insights into a wide range of physiological parameters, making it an indispensable tool in both disease diagnosis and monitoring.

However, conventional blood collection and analysis methods require relatively large sample volumes (~7.5mL), involve invasive procedures, and require extensive laboratory pre-processing. Additionally, these methods are often time-consuming and rely on complex equipment, which makes them unsuitable for routine diagnosis and monitoring within primary healthcare. In this context, the ability to perform point-of-care (PoC) diagnostic tests is crucial to ensure timely clinical interventions, promoting therapeutic efficacy and improving healthcare.

To address these limitations, microfluidic technologies offer a promising alternative, enabling the minimally invasive processing of blood samples (*e.g.* a drop of capillary blood) in compact and miniaturized devices. In particular, microfluidic systems can facilitate the extraction of plasma from whole blood in microlitre range, eliminating the need for extensive external pre-processing.

Thus, this dissertation aims to optimize the use of a microfluidic chip to enable and maximize plasma extraction from a small capillary blood sample obtained via finger prick. This chip consists of a Luer interface to load the blood sample, a support channel, a 10 mm diameter filtration membrane, a plasma collection channel, a ventilation channel and interfaces for vacuum application and pressure relief. In addition to the chip, complementary accessories are used, such as a reservoir for sample loading and a male mini Luer plug for proper interface control. To achieve the proposed objective, experiments are conducted to evaluate key variables, including the capillarity of the chip, the mechanical force applied to the complementary components, as well as testing different levels of capillary blood dilution (undiluted, 1:2 and 1:4) to determine the most effective approach. The mechanical force consists of opening the third interface, while simultaneously applying vacuum to the second interface using a syringe. A pipette was also employed for a similar purpose. Manual thumb pressure on the reservoir lid or the repeated insertion and removal of the male mini Luer plug from the lid are also examples of mechanical force applied to the system. After multiple trials, results indicate that the most effective approach for plasma extraction consists of using whole blood diluted at 1:4 ratio, combined with one of the previously mentioned methods of applying manual pressure to the reservoir.

By eliminating invasive blood collection and rapid processing, while avoiding hemolysis and chip clogging, this miniaturized microfluidic system represents a significant step toward the development of

an integrated, all-in-one diagnostic platform. In the future, such technology could enable rapid, cost-effective, and accessible PoC testing by simultaneously processing, analyzing, and quantifying molecular biomarkers *in situ*, related, for example, to maternal-fetal health, enabling health monitoring of the mother and the baby to be carried out more quickly and affordably at the PoC.

**Keywords:** Microfluidic Chip, Blood-Plasma Extraction, Primary Health Care, Diagnosis

# TABLE OF CONTENTS

Copyrights and conditions of use of this work by third parties ..... i
Acknowledgements ..... ii
Statement of integrity ..... iv
Resumo ..... v
Abstract ..... vii
Table of contents ..... ix
List of figures ..... xi
List of tables ..... xiv
List of abbreviations and acronyms ..... xv
1. Introduction ..... 1
1.1 Context ..... 1
1.2 Objectives ..... 3
1.3 Document structure ..... 3
1.4 Research's outcomes ..... 4
2. Literature review ..... 5
2.1 Blood as a diagnostic fluid in medical diagnostics ..... 5
2.2 Current limitations in pre-analytical blood processing ..... 7
2.3 The gold-standard mechanical method for blood-plasma separation ..... 9
2.4 Introduction to microfluidics: key concepts and design considerations ..... 12
2.5 Blood-plasma separation techniques used in microfluidic chips ..... 16
2.5.1 Active techniques: theorical principles ..... 17
2.5.2 Passive techniques: theorical principles ..... 23
2.5.3 Representative studies on active microfluidic techniques for blood-plasma separation ..... 26
2.5.4 Representative studies on passive microfluidic techniques for blood-plasma separation 33
2.5.5 Hybrid methods ..... 40
3. Materials and methodologies ..... 44

3.1 Materials ..... 44
3.1.1 Devices and Components ..... 44
3.1.2 Reagents ..... 44
3.1.3 Biological samples ..... 45
3.2 Fluidic 168: specifications and experimental approach ..... 45
3.2.1 Microfluidic optimization procedure: methodology adopted ..... 47
4. Experimental results and discussion ..... 54
4.1 Experimental results ..... 54
4.2 Discussion of the experimental results ..... 55
4.2.1 First method tested: pressure equalization and vacuum application ..... 55
4.2.2 Second method tested: pre-run with PBS and outlet suction via pipette ..... 55
4.2.3 Trials with diluted capillary whole blood ..... 55
4.2.4 Assessing plasma separation performance ..... 57
4.2.5 Comparison of the Fluidic 168 chip performance with the aforementioned literature ..... 58
5. Conclusion and future perspectives ..... 60
5.1 Conclusions ..... 60
5.1.1 Objectives' Fulfilment ..... 61
5.2 Future Perspectives ..... 62
6. References ..... 65

# LIST OF FIGURES

Figure 1: Blood components. Created with Biorender and inspired from [2]. ..... 6
Figure 2: The main phases of the testing process. Created with Biorender and inspired from [15]. ..... 7
Figure 3: Order of draw and the respective color-code, additives and applications [17], [18], [19]. Created with Biorender. ..... 8
Figure 4: Procedure performed to obtain plasma and serum samples from whole blood. Created with Biorender. ..... 11
Figure 5: Different blood behaviours: (a) RBCs aggregation; (b) CFL region [33]. ..... 15
Figure 6: Blood-plasma separation techniques. Created with Biorender and inspired from [40]. ..... 17
Figure 7: Illustration of magnetophoresis. It illustrates the displacement of particles either toward the magnetic field (indicated by the blue vector) or away from it (indicated by the red vector). This movement is governed by the difference in magnetic susceptibility between the particle ($Xp$) and the surrounding medium ($Xf$) [42]. ..... 18
Figure 8: Illustration of magnetophoresis with labelled target with magnetic beads [43]. ..... 19
Figure 9: Illustration of capture-based separation: (a) Introduction of magnetic beads; (b) Trapping magnetic beads with a magnet; (c) Introduction of a sample containing target cells; (d) The target cells are captured; (e) The magnet is removed to release the target population of cells [43]. ..... 19
Figure 10: Illustration of continuous-flow magnetophoresis [43]. ..... 20
Figure 11: Illustration of acoustophoresis [43]. ..... 20
Figure 12: Illustration of the separation of a heterogeneous sample via acoustophoresis: (a) Heterogeneous sample (red and green particles); (b) The sample is exposed to an acoustic field; (c) Due to acoustic contrat factor, red and green particles move toward different positions; Green particles are moved toward the sidewall antinodes and the red particles move toward the central node [43]. ..... 21
Figure 13: Illustration of dielectrophoresis [43]. ..... 22
Figure 14: Multistep and continuous DEP: (a) Retention; (b) Migration; (c) Deflection [43]. ..... 23
Figure 15: Illustration of dead-end and cross-flow filtration. Edited from Figure 3 from [30]. ..... 24
Figure 16: Illustration of sedimentation-based technique for plasma separation. Edited from Figure 3 in [30]. ..... 24
Figure 17: Illustration of the lateral displacement technique. Edited from Figure 2 in [40]. ..... 25

Figure 18: Illustration of hemodynamic effect- Bifurcation Law. Adapted from Figure 2 in [40]..... 26
Figure 19: (a) Diamagnetic blood-plasma separation from undiluted whole blood device using SPIONs: (i) Cross section of the system and (ii) Schematic of the device [50]; (b) Power-free device for plasma separation based on negative magnetophoresis: (i) Visual representation of the experimental setup and (ii) Schematic diagram of the system. Adapted from [51]..... 28
Figure 20: (a) Microfluidic for blood-plasma separation and detection of biomarkers using acoustic microstreaming: (i) Design of the system and (ii) Images demonstrating the plasma separation at different locations of the device. Adapted and edited from [52]; (b) Impedance mismatch-assisted acoustofluidic device: (i) Schematic of the system; (ii) Left, acoustic transducer off: whole blood is collected at the lower outlet. Right, transducer on:blood cells are separated to the upper outlet, when a sheath fluid is introduced [53]..... 31
Figure 21: Dielectrophoretic microfluidic chip for plasma separation: (a) Schematic of the system; (b) RBCs are dispersed when the voltage is off; (c) Voltage on:Positive DEP drives RBCs to the surface; (d) While plasma flows over time, RBCs remain aggregate. Adapted from [54]. ..... 32
Figure 22: (a) Circular gradient-width crossflow plasma separation device: (i) Top view; (ii) Comparison of traditional straight crossflow vs. new developed curved, gradient-width crossflow design [31]; (b) Filtration-based microfluidic chip: (i) Adhesive was cut to include an inlet well, outlet well, and a channel connecting them and filtration membrane placed over inlet well. Whole blood (red) is applied onto the filter; (ii) Plasma path indicated by arrows. Adapted from [29]. ..... 35
Figure 23: Operational principles of PPS-V2 system with SPR biosensor: (a) The PPS-V2 device assembled with membrane; (b) Schematic of the side view, exhibiting three PDMS layers and a membrane. The blood flows by capillary channels; (c) Top view of layer 3 design: capillaries, a capillary micropump and outlet reservoirs. Adapted and edited from [55]. ..... 37
Figure 24: Plasma separation device through hemodynamic phenomena: (a) Schematic and dimensions of the system; (b) Illustration that demonstrates how cells flow through CEA and form the CFL [56]. .. 38
Figure 25: Microfluidic chip based on deterministic lateral displacement: (a) Dimensions and elements of the microfluidic chip; (b) Crescent-shaped filter and detailed schematic of its configurations. Five filters blocks positioned with gradually increasing gaps (h1-h4) and each filter block began with the smallest pillar size (Q1), followed by larger pillars (Q2-Q4). Adapted and edited from [46]..... 39
Figure 26: DMF blood-plasma separation: (a) Connection to the system unit; (b) Whole blood is loaded on the SM, where RBCs are trapped. Plasma flows to the electrode array, passing through the TM. Then

the buffer is added to help collection; (c) Buffer moves across the membrane, pulling plasma with it into a droplet; (d) Plasma is inside the droplet and can be tested [57]. ..... 42
Figure 27: Microfluidic device to extract plasma from undiluted whole blood by gravitational sedimentation: (a) Left: prototype and right: schematic of the microsystem; (b) Working principle of the device- through nDEP force, cells flow to the bottom of the channel and are guided into the separation trench. Here gravity ($Fgb$) acts on cells. The trench is sealed with MBPP layer, while plasma flows on top. Adapted and edited from [45]. ..... 43
Figure 28: Schematic representation of the chip Fluidic 168 [58]. ..... 46
Figure 29: Close-of photograph of the plasma generation chip Fluidic 168 elements [60]. Edited with Canva. ..... 47
Figure 30: Decision digrama followed in the first attempt-methodology. ..... 49
Figure 31: Decision digrama followed in the second attempt-methodology. ..... 49
Figure 32: Decision digrama followed in the third and fourth attempt-methodology..... 52
Figure 33: Decision digrama followed in fifth attempt-methodology. ..... 52
Figure 34: Decision digrama followed in the sixth attempt-methodology. ..... 53
Figure 35: Photograph showing the application of mechanical force using the thumb to load the sample. ..... 56
Figure 36: Photographs of the steps followed to load one of the samples: (a) Open the reservoir lid; (b) Inject the sample; (c) Remove the male mini Luer plug at the second interface; (d) Apply mechanical force with the finger to load the sample and (e) Collect the sample. ..... 57
Figure 37: Plasma solution obtained by loading 1:4 diluted whole blood. ..... 57
Figure 38: Power-free, weight-induced vacuum platform for plasma separation. Created with bioreneder. (a) Structure of the system; (b) Blood sample's weight creates a downward force, making the plunger descend. Vacuum is created, being the blood drawn into the support's channel. ..... 63

# LIST OF TABLES

Table 1: Lexicon of terms used at the microfluidic field [30]. ..... 15
Table 2: Forces and operational mode applied in initial trials-undiluted capillary blood sample- -to optimize the microfluidic chip. ..... 48
Table 3: Samples along with the corresponding reagents and volumes used for preparing each solution to evaluate and optimize the plasma extraction microfluidic chip. ..... 51
Table 4: Forces and operational mode applied in whole blood samples with different dilution levels. .. 51
Table 5: Results achieved in each trial with the respective forces and operational mode. ..... 54

# LIST OF ABBREVIATIONS AND ACRONYMS

| | |
|---|---|
| **AC** | Alternating Current |
| **BEST** | Biomarkers, Endpoints and Other Tools |
| **CD** | Centrifugal Disk |
| **cDEP** | Contactless Dielectrophoresis |
| **CFL** | Cell-Free-Layer |
| **CFD** | Computational Fluid Dynamics |
| **CuACE** | Copper-Assisted Chemical Etching |
| **DC** | Direct Current |
| **dd$H_2O$** | Double Distilled Water |
| **DEP** | Dielectrophoresis |
| **DLD** | Deterministic Lateral Displacement |
| **DMF** | Digital Microfluidic |
| **DNA** | Deoxyribonucleic Acid |
| **EDTA** | Ethylenediaminetetraacetic Acid |
| **ELISA** | Enzyme-Linked Immunosorbent Assay |
| **HCHTPS** | Hydrodynamic Continuous High-Throughput Plasma Separator |
| **KCl** | Potassium Chloride |
| **KOH** | Potassium Hydroxide |
| **LOD** | Limit of Detection |
| **LOQ** | Limit of Quantification |
| **MBPP** | Melt-Blown Polypropylene |
| **MR** | Measles Rubella |
| **PBS** | Phosphate Buffered Saline |
| **PDMS** | Polydimethylsiloxane |
| **PoC** | Point-of-Care |
| **PSA** | Prostatic Specific Antigen |
| **PZT** | Piezoelectric |
| **RBCs** | Red Blood Cells |
| **RT** | Room Temperature |
| **RV** | Rubella Virus |
| **SPION** | Superparamagnetic Iron Oxide Nanoparticles |
| **SPR** | Surface Plasmon Resonance |

| | |
|---|---|
| **Vpp** | Voltage Peak to Peak |
| **WBCs** | White Blood Cells |
| **WHO** | World Health Organization |

CHAPTER 1

# 1. INTRODUCTION

This section provides an overview of the project, outlining its primary goals, relevance, and expected contributions. Additionally, it presents the structure of this document, offering a clear roadmap for the reader to understand the logical progression of the research.

## 1.1 Context

Blood is a complex biological fluid composed of various cellular components, including erythrocytes, lymphocytes and platelets, which are suspended in plasma. This transport medium is rich in proteins, ions, dissolved gases, nutrients and metabolic products [1], [2]. Within the diverse constituents of blood, cellular elements, genetic material, and proteins are all recognized as potential biomarkers [3], [4]. According to the Biomarkers, Endpoints, and other Tools (BEST) resource, a biomarker is a characteristic that is measured and evaluated to indicate normal biological processes, disease states, or responses to exposures or treatments [5]. Among various bodily fluids, blood is widely regarded as the gold standard for providing comprehensive diagnostic information about an individual's physiological and pathological state. This is because blood contains a diverse range of components that reflect the body's overall health [1]. By analyzing its components, biomarkers can be identified and used to improve the precision of disease diagnosis, prognosis, and therapeutic monitoring. Consequently, incorporating biomarkers into clinical development and treatment strategies enhances the accuracy of patient assessment and increases the likelihood of successful outcomes [5].

Blood tests ordered by doctors undergo multiple stages before the results are communicated to the patient [3]. The overall process of blood testing includes pre-analytical, analytical and post-analytical steps [1]. The pre-analytical stage includes all procedures from blood sample's collection to preparation [1], which this last may involve, for example, centrifugation for blood separation, in which plasma and serum are isolated for diagnostic purposes [2], [6]. The following stage encompasses blood sample's analysis, in which biomarkers are detected. However, each of these steps has its own challenges and limitations. Blood is normally collected through venipuncture, a highly invasive procedure that can be harmful for patients. Moreover, the considerable volume of blood drawn generates biological waste, and

phlebotomists are at risk of developing infections due to needlestick injuries. This method also requires skilled professionals and specialized laboratory equipment [1]. As previously noted, blood is a complex biological matrix comprising multiple components, each with distinct diagnostic relevance; consequently, the sample preparation stage is of critical importance [2], [6], [7]. This stage involves steps to separate relevant blood components (such as plasma, serum, or cellular fractions) and to reduce potential interferences that could affect the accuracy and reliability of analytical testing. The specific preparation protocols vary depending on the target analyte, sample type, and selected analytical method [2].

A widely used separation technique is centrifugation, which is the standard method for plasma and serum extraction. However, centrifugation requires trained personnel, can be time-consuming, and depends on sophisticated equipment that needs regular maintenance and calibration [2]. Similarly, biomarker detection is often performed using the enzyme-linked immunosorbent assay (ELISA) [8], a well-established immunoassay technique. ELISA shares several limitations with centrifugation, including the requirement for expensive and complex instrumentation, as well as lengthy blocking and incubation steps necessary to complete the assay [9]. Overall, the process of whole blood collection and analysis can be labor-intensive and time-consuming, often requiring several days to weeks before results are available. Such delays in diagnosis and treatment initiation may prolong disease progression due to the lack of timely intervention. In severe cases, this lag can contribute to deterioration of the patient's condition and may increase the risk of morbidity or mortality [1], [10].

Considering the challenges previously discussed, several research teams have focused on advancing blood sample preparation by developing innovative techniques that automate these procedures, thereby reducing sample handling time and improving efficiency [2]. This has led to the emergence of microfluidic technologies, which operate at the microscale by confining small volumes of liquids or gases within microchannels [2]. These systems offer significant advantages, including automation that minimizes human intervention, reduced reagent consumption [8], and enhanced portability.

Microfluidic systems have played a key role in the evolution of point-of-care (PoC) testing, enabling real-time medical diagnosis outside traditional laboratories settings [8]. This advancement is particularly valuable in resource-limited regions, where access to conventional diagnostic facilities may be restricted. By integrating microfluidic technologies with PoC testing, it becomes possible to achieve rapid and cost-effective clinical detection, ultimately improving healthcare outcomes while reducing financial and logistical burdens.

Considering these aspects, the motivation behind this project is to optimize microfluidic chip procedures for PoC finger-prick blood-plasma extraction. By achieving this, it is possible to avoid sample

preparation off-chip and the invasive blood collection. In future research, integrating this microfluidic chip with a detection system could enable faster result acquisition, facilitating earlier therapeutic interventions and improving patient care.

## 1.2 Objectives

This project aims to optimize a microfluidic chip procedure for PoC blood-plasma extraction. To achieve this goal, the objectives were divided into the following key steps:

- **Objective 1:** Develop and optimize a protocol for the rapid and efficient processing of finger-prick blood using a miniaturized microfluidic chip.
- **Objective 2:** Conduct preliminary tests to refine the plasma extraction process and assess potential hemolysis during sample loading.
- **Objective 3:** Evaluate the efficiency of plasma extraction using the microfluidic chip.

By meeting these objectives, the project seeks to establish a reliable method for plasma extraction, contributing to the advancement of integrated PoC diagnostic solutions.

## 1.3 Document structure

This document is structured into the following chapters, as described below:

Chapter 1- Introduction: To establish a comprehensive understanding of the topic, the first chapter presents the background and motivation behind this study. It highlights the relevance of developing and optimizing a microfluidic chip procedure for PoC blood-plasma extraction, emphasizing its potential impact on diagnostic techniques and healthcare advancements.

Chapter 2- Literature Review: The second chapter provides the theoretical foundation for this research, presenting key concepts related to blood analysis and microfluidic technology. It begins by discussing the significance of blood in medical diagnostics, explaining its role as a valuable source of biomarkers and its widespread use in clinical analysis. Additionally, it examines conventional techniques for blood sample processing, highlighting their methodologies, advantages, and limitations. Furthermore, this chapter explores the importance of miniaturization in diagnostic applications, emphasizing how microfluidic technologies are revolutionizing PoC testing. It presents different types of microfluidic devices designed for plasma extraction, detailing their working principles and comparing their benefits to

traditional blood processing techniques. The advantages of these miniaturized systems, such as reduced sample volume, faster processing times, and enhanced accessibility, are also discussed.

Chapter 3- Materials and Methodologies: The third chapter details the experimental procedures undertaken to optimize the microfluidic chip for blood-plasma extraction. It describes the step-by-step development of the experimental setup, including the materials, reagents, and protocols employed. Furthermore, this chapter outlines the systematic approach used to assess and refine the chip's performance, ensuring its efficiency and reliability for PoC applications.

Chapter 4- Experimental Results and Discussion: This chapter presents the results obtained from the experimental work described in the previous section and it provides a critical analysis of the findings.

Chapter 5- Conclusions and Future Perspectives: The final chapter summarizes the key conclusions drawn from the present study, reflecting on the accomplishment of the project's objectives. It also presents potential improvements and future directions for this research, emphasizing the remaining challenges and the necessary steps for further advancements in microfluidic-based blood-plasma extraction. These future perspectives are crucial in guiding subsequent research efforts and potential clinical applications.

## 1.4 Research's outcomes

**Publications:**

Estrela, D., **Santos, R. F.**, Masserdotti, A., Silini, A., Parolini, O., Pinto, I. M., & Cruz, A. (2025). *Molecular Biomarkers for Timely and Personalized Prediction of Maternal-Fetal Health Risk*. Biomolecules, 15(3), 312. doi: 0.3390/biom15030312.

**Conferences and Workshops:**

- Workshop I: Regulations, policy and exploitation, 11th June 2024 at Institute for Research and Innovation in Health, University of Porto-9:00 am to 17:40 pm;
- LIFESAVER Conference (Living impact on fetal evolution), 13th June 2024 at Institute for Research and Innovation in Health, University of Porto-9:00 am to 17:30 pm;
- Workshop II: Exploitation of R&D results, 14th June 2024 at Institute for Research and Innovation in Health, University of Porto-9:00 am to 16:40 pm.

CHAPTER 2

# 2. LITERATURE REVIEW

The purpose of this chapter is to provide an overview of the main topics of this project. It will explore themes such as the importance of whole blood in medical diagnostics and its barriers in the analytical phase of blood processing. Furthermore, it will cover the conventional techniques for blood sample processing and how microfluidic came to overcome the limitations brought by the traditional methods. Finally, it will highlight examples of microfluidic systems for plasma extraction.

## 2.1 Blood as a diagnostic fluid in medical diagnostics

Blood is the most extensively studied body fluid for diagnosis [1], [10]. It plays several key roles in our body, including heat distribution, transportation of various substances, immune cell defence, and the maintenance of acid-base balance and osmotic equilibrium [11]. Blood is a complex fluid, comprising both cellular and acellular components [12]. Plasma, which is yellow in colour [11] is included in the acellular category [12], and comprises 90% of water and 7% of proteins (e.g. albumin, fibrinogen, globulins). The remaining 2% and 1% are organic elements (e.g. aminoacids, vitamins, hormones, lipoproteins) and inorganic salts, respectively [11]. The cellular components of blood include various blood cells, such as erythrocytes (red blood cells, RBCs), thrombocytes (platelets), and leukocytes (white blood cells, WBCs). The RBCs are non-nuclear, circular cells with a biconcave shape and typically have a diameter of 6-8 μm [11],[13]. However, variations exist. Larger RBCs, known as macrocytes, have diameters greater than 8 μm [11], while smaller RBCs, termed microcytes, measure less than 6 μm in diameter [11],[14]. These type of blood cells delivers hemoglobin, which transports oxygen to cells and are also composed by blood grouping antigens [2]. Additionally, thrombocytes, also known as platelets, are non-nucleated cells that come from bone marrow. These type of blood cells are 1-5 μm in diameter [11], [14]. In addition, some platelets are classified into two subgroups, the large platelets (diameter of 4-7 μm, [11]) and the giant platelets (diameter of 8-20 μm, [11]). WBCs are nucleated cells that serve as the body's defenders. In the blood, they appear spherical but vary in structure, nuclear shape, and size [11]. Leukocytes are further classified into granulocytes and agranulocytes, depending on the presence or absence of granules, respectively [11]. Granulocytes include neutrophils (10-12 μm in diameter), eosinophils (12-14 μm in diameter), and basophils (9-10 μm in diameter). In contrast, the

agranulocytes group consists of small, medium, and large lymphocytes (6-8 µm, 10-12 µm, and 8-18 µm in diameter, respectively) and monocytes (12-20 µm in diameter) [11]. In terms of composition, blood consists of approximately 54% plasma and about 45% red blood cells. After centrifugation, a buffy coat appears between RBC's and plasma layers, where leukocytes and platelets are found, making up less than 1% [2]. Figure 1 presents the constitution of blood and the respective percentages.

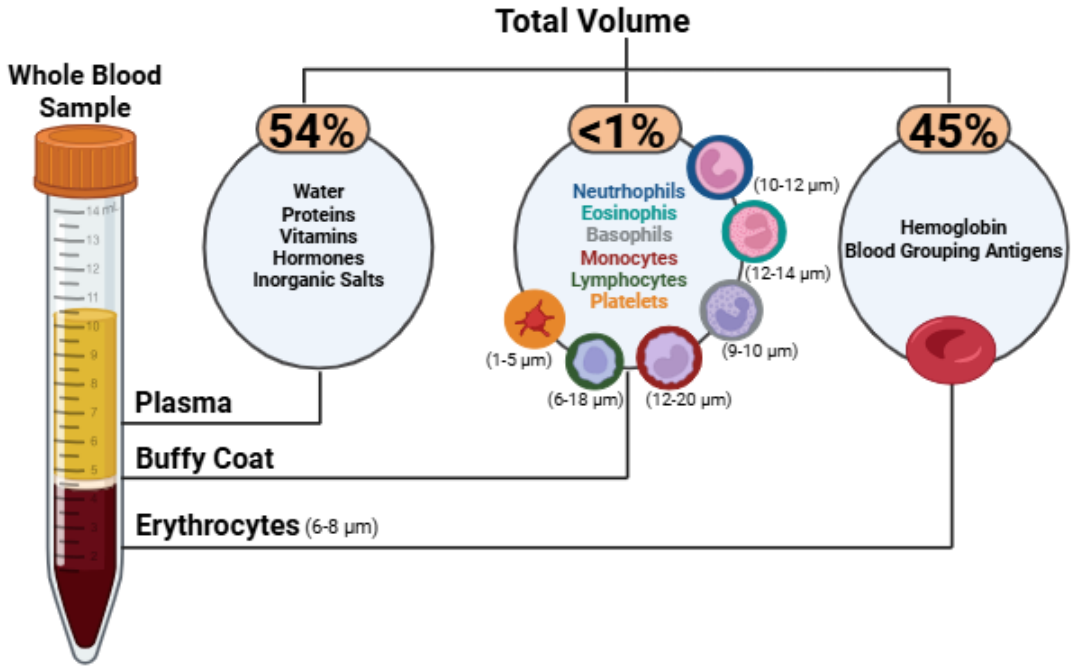



**Figure 1:** Blood components. Created with Biorender and inspired from [2].

Specific cells, genes and proteins found in blood can be classified as biomarkers [3], [4]. As referred previously, accordingly to BEST, a biomarker is a "characteristic that is measured as an indicator of normal biological processes, pathogenic processes, or responses to an exposure or intervention, including therapeutic interventions." Examples of them are the predictive and the prognostic biomarkers. The first category serves to identify patients who are more likely to respond favorably to a specific therapeutic intervention, minimizing the risk of adverse reactions in patients with adverse outcomes. Furthermore, prognostic biomarkers are useful for estimating the likelihood of subsequent clinical occurrences in a disease [5]. Various tests have been developed to identify and quantify numerous biomarkers such complete blood counts, the quantification of vitamin D and hormone levels [2]. Therefore, through the analysis of a blood sample or its various components it is possible to examinate an individual's organ functions and various other health indicators, being this fluid considered the most diagnostically sample

matrix [1]. From the moment a blood test is ordered to the confirmation of a specific diagnosis, whole blood samples undergo a complex, multi-step process [3], which will be detailed in the following subchapter.

## 2.2 Current limitations in pre-analytical blood processing

The total blood testing process can be divided into three stages: pre-analytical phase, analytical phase and post-analytical phase. The pre-analytical phase encompasses sample's collection, handling, transportation, storage and preparation [1]. Examples of sample preparation techniques are dilution, cell lysis [2], filtration and centrifugation, for plasma and serum separation from whole blood [6], as mentioned earlier. In addition, sample analysis is included in the second phase, while the third phase covers test validation, interpretation and the report of the results to the patient [1]. Figure 2 presents the steps behind the testing process of a blood sample. Although, this subchapter will focus solely on the initial phase of the process, up to the point of storage.

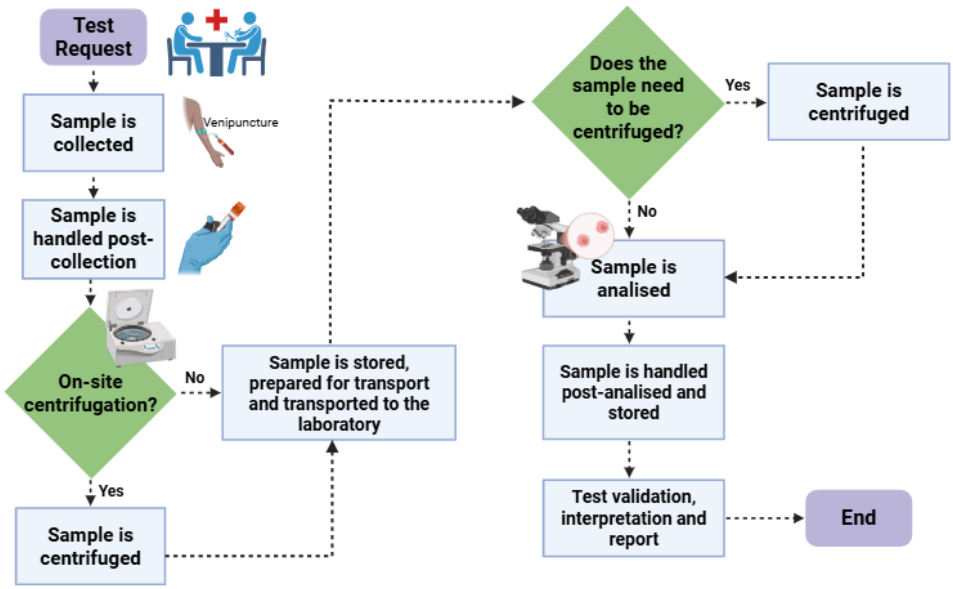



**Figure 2:** The main phases of the testing process. Created with Biorender and inspired from [15].

In sample collection stage, whole blood is collected by trained professionals [1], via venipuncture and placed into sterile tubes [2], coated with some additives suitable for a particular application. In addition, the healthcare professionals execute restricted protocols to collect blood, being the tubes distinguished by their color-code stoppers and drawn in a certain order to avoid cross-contamination of

additives [16]. The color-code, the respective applications and additives of the tubes are presented in Figure 3.

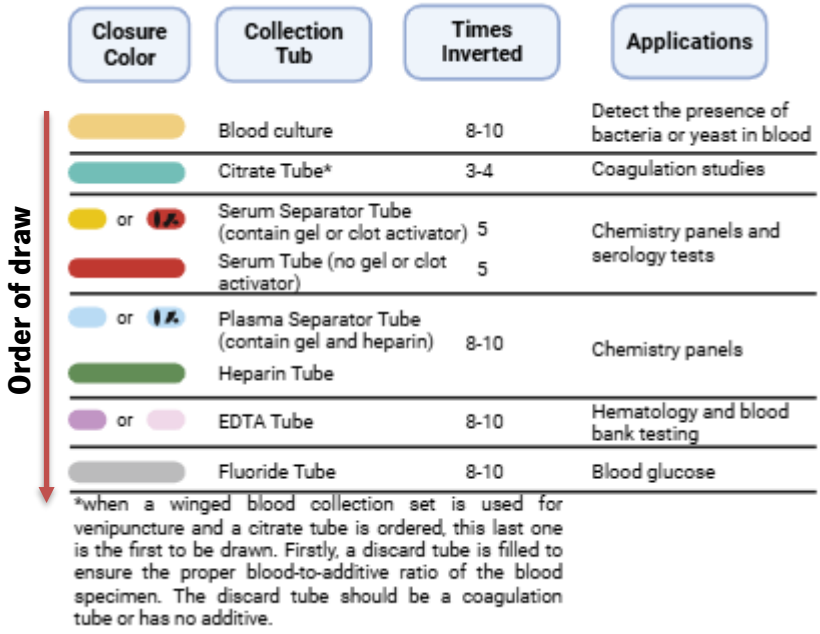



**Figure 3:** Order of draw and the respective color-code, additives and applications [17], [18], [19]. Created with Biorender.

For instance, if the lavender tube is taken out before the gold tube is collected, the potassium would rise [20], interfering with results. It is important to notice that color-code and the additives used may vary, so it is crucial to verify the protocol followed by the institution in question [21]. Among the additives used, are anticoagulants which need to be cautiously chosen to avoid problems in certain applications [16]. Examples of them include ethylenediaminetetraacetic acid (EDTA), citrate or heparin, differing in their mode of action. The first two bind to calcium ions, which are responsible for the induction of coagulation factors and platelets. On the other hand, heparin binds to antithrombin, activating it. Consequently, all the previous anticoagulants prevent blood from clotting, keeping it in its liquid form, being easier to handle and conserving its composition [2]. Moreover,when collecting blood, the tubes need to be gently inverted. For example, while phlebotomist collects a new sample, they can invert the previous tube. Although, if the professional is not able to invert the vacutainer while the other bottle is filling with blood, then the phlebotomist inverts all the tubes, after the collection of all samples [22]. Each type of tube has a recommended number of times to be inverted specified in the recommendations [21]. In general, all

tubes should be inverted at least five to ten times to mix the content, except the tube containing sodium citrate, which may be inverted three or four times [20] (Figure 3). This step is important and must be executed carefully, since when performed incorrectly could lead, in some samples, to erythrocyte damage. Consequently, hemolyzed specimens have the potential to interfere with some optical instruments and create chemical interferences [23].

In addition, blood tubes should be transported closed and in a vertical position, which allows the clot formation and minimizes agitation of the content, which consequently prevents hemolysis. Additionally, some samples include analytes photosensitive and should not be exposed to artificial light and sunlight [23]. Furthermore, as previously mentioned, all blood samples must be considered infectious, being for this reason transported in a sealed biohazard bag. In addition, another crucial variable to be considered is the temperature in which blood samples are stored before, during and after the courier pickup. As an example, accordingly to *Lexington Medical Center*, the specimens are kept in a sealed orange/red biohazard labelled bag if there are no special storage needs and the sample will be kept at the room temperature (RT) prior to courier pickup. On the other hand, if the specimens need refrigerated temperatures during transport, they are kept in a blue biohazard bag. Therefore, this color will inform the courier that the sample must be transported on ice. Finally, if a specimen must be frozen after processing, it needs to be centrifuged firstly and then separated in labelled aliquote tubes. After this step and until the collection, the specimen will be placed on dry ice or in a freezer, inside a blue biohazard bag as previously referred. In some cases, red biohazard bags with "STAT" written are used, which informs the courier to the urgence of the transport [20].

In the next subchapter will address the following step of the pre-analytical phase-preparation of blood sample.

## 2.3 The gold-standard mechanical method for blood-plasma separation

The preparation of whole blood samples is a critical component of the analytical workflow, serving as the bridge between sample collection and analysis. Due to the complex composition of whole blood [1], including cellular components and potentially interfering substances, whole blood requires careful preparation to allow accurate identification and quantification of target analytes. Depending on the type of test to be performed, blood can be processed into different sample types- plasma and serum [2]. Therefore, appropriate sample preparation methods are essential to eliminate interfering substances,

isolate the analytes of interest and improve their detectability, all of which contribute to reliable and repeatable analytical results [6].

Among the preparatory procedures, this subchapter will focus specifically on centrifugation, which remains the gold- standard mechanical method employed for actively separating plasma from whole blood in a laboratory setting [1], [2], [6], due to its high efficiency. However, recent advances in microfluidics, membrane filtration, and acoustofluidics have enabled alternative separation techniques suitable for various settings, including point-of-care diagnostics. These methods exploit different physical principles—such size-based filtration, acoustic radiation forces and microscale flow dynamics, to obtain plasma with varying degrees of purity and yield. These information will be discussed in detail later in subsection 2.5. While plasma is the primary focus in this work, it is worth mention that serum can also be obtained through centrifugation, using a different procedure.

In the context of centrifugation, to obtain plasma, the whole blood sample is collected in tubes containing anticoagulant [2]. After collection, the tubes of plasma must be placed in a rack at room temperature and be centrifuged within 2 h of collection [24]. Consequently, after centrifugation, the sample is separated into plasma (upper layer), followed by a buffy coat , including WBCs and platelets (middle layer). Finally at the bottom, RBCs are sedimented [2]. This can be seen in Figure 4, left panel. On the other hand, obtaining serum requires blood collection without anticoagulant. The tubes must be allowed to clot, at room temperature for a minimum of 30 min before centrifugation [24]. Ideally, centrifugation is performed within 1 h of collection and no later than 2 h after complete clotting [20]. The result, after centrifugation, is serum at the upper layer, visible as yellow (Figure 4, right panel) [2]. Serum differs from plasma by lacking fibrinogen and certain coagulation factors [2].

In addition, concerning to the mechanism of centrifugation itself, the tubes of the samples are collected and rotate at high speeds, being the common centrifugation techniques dependent on various features of cells, including size and density [25]. Among the centrifugation methods are the differential centrifugation and the density gradient centrifugation [26]. In the first referred technique, the cells are combined with an isotonic buffer or growth medium and sediment at diverse rates. The compounds with higher size and density, sediment faster followed by the smaller size and less dense ones. In differential centrifugation, the medium used is homogeneous.

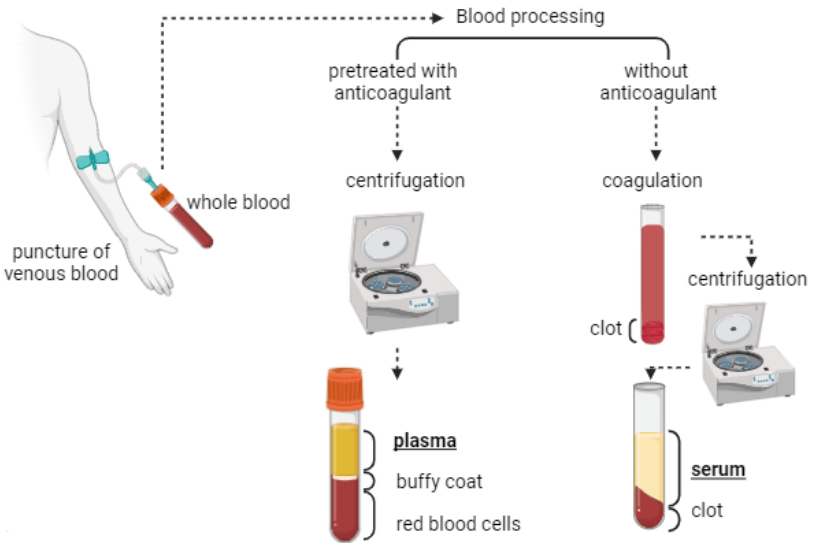



**Figure 4:** Procedure performed to obtain plasma and serum samples from whole blood. Created with Biorender.

For this reason, only two fractions can be produced: a cell pellet at the bottom of the tube and a portion of cells in the liquid above the pellet, designated as supernatant [27]. Additionally, to achieve a faster sedimentation rate of the particles, the gravitational force can be increased. However, the g-force required to pellet the larger cells is also sufficient to pellet the tiniest ones, leading to the inclusion of smaller cells in the pellet formation [27]. To address this, centrifugation can be performed in multiple steps, with the supernatant subjected to progressively higher speeds. This method improves separation because the smaller particles remain in the supernatant until they are sedimented in a later stage, achieving more purified samples. In addition, differential centrifugation is often used to separate macromolecules, cell organelles and for simple pelleting [26]. On the other hand, in the density gradient method, the homogeneous medium is replaced by a solution, which increases the density along the tube. Moreover, rate-zonal and isopycnic are two types of density gradient centrifugation variations. In the first variation, the compounds are centrifuged and the cells with different sizes sediment at various rates, similar to differential centrifugation. However, in this technique, the centrifugation is performed through a density gradient, which increases down the tube, but never surpasses the density of the cells in question. As a result of this density gradient, cells of equal sizes sediment together as a band. However, all cells can form a pellet if the centrifugation is carried out for a long period of time, due to the increased density of cells compared to the medium, being this technique time-dependent. In the isopycnic method, unlike the previously discussed technique, the density of the gradient exceeds that of the target cells. In this method, cells sediment at the point where their density matches that of the gradient. Additionally, the compounds form distinct bands and do not reach the bottom of the tube, as the surrounding medium has a higher

density [27]. When considering centrifuges, it is essential to account for the heat generated during operation, as it may compromise the stability of temperature-sensitive analytes. [23]. Conversely, certain whole blood samples do not require separation and are therefore not subjected to centrifugation.

Centrifugation, while effective for blood processing, presents several limitations. It is a time-consuming process that requires specialized staff, a laboratory setting, and regular maintenance [2]. Furthermore, the equipment used for centrifugation is often complex, large, and expensive, making it unsuitable for point-of-care (PoC) applications [28]. In laboratories, whole blood is typically collected via venipuncture, with volumes of approximately 7.5mL per tube. This method, although standard, is invasive and can be uncomfortable for patients [1]. Additionally, these large volumes are not characteristic from PoC diagnostics, such finger pricks [28]. Furthermore, traditional centrifugation can sometimes lead to red blood cell lysis, releasing hemoglobin that may compromise test accuracy [2].

According to the World Health Organization (WHO), an ideal diagnostic method for PoC should be affordable, sensitive, specific, rapid, user-friendly, equipment-free, and robust [29]. For PoC testing to be effective, plasma must be extracted from whole blood maintaining protein integrity, ensuring accurate biomarker detection without interference from blood cells. To address these limitations, microfluidic systems have been developed as an alternative, offering a solution where traditional centrifugation is not practical for PoC settings.

## 2.4 Introduction to microfluidics: key concepts and design considerations

As referred previously, centrifugation techniques are not compatible for PoC diagnostics, being a considerable part of blood preparation performed manually and off-chip [30]. Consequently, researchers have focused on developing microfluidic devices capable of performing plasma separation using various techniques. Before introducing this topic, this subchapter will address the theoretical foundations of microfluidics and discuss several critical design factors that ensure efficiency in developing microfluidic systems for plasma separation.

Microfluidic devices work with dimensions at the micron range, processing fluids with small volumes with microscale channels [29]. One practical example is the use of the finger prick blood collection, characterized as a minimally invasive method which eliminates the need for phlebotomists [2] and reduces patients' pain [1]. Furthermore, some automated microfluidic approaches do not need specialized training [30]. In addition, for small sample volumes, microfluidic devices advantages include

portability [31], allowing the transportation to the patient bedside or to the doctor's office [30]. Additionally, these systems offer other benefits such as rapid evaluation and low price per device [32]. Thus, contrary to centrifugation, microfluidic devices are suitable for PoC diagnostics [29]. Still, there are some limitations that need to be addressed at the microfluidic systems' field. The following paragraphs outline representative challenges faced by designers of microfluidic devices for plasma separation, such as constraints related to sample volume, variability in hematocrit levels, clogging risks, biocompatibility of materials and the product life cycle of the systems.

### Sample Volume

Although achieving miniaturization is a key goal in microfluidic systems' design, it does not imply the reduction of the sample volume. The collected sample must be representative of the target analyte, despite smaller systems often enhance sensitivity. Two distinct volumes that are considered for blood collection are the capillary samples and venous samples. While the first example includes volumes in the microliter range, collected from fingertips (~10 μL), the second one comprises larger volumes obtained by venous puncture (1-50 mL) [30].

### Hematocrit Level

Hematocrit is related to the volume percentage of RBCs in blood [30]. Elevated hematocrit levels in certain samples can lead to clogging of microchannels and membranes, thereby obstructing analytes from reaching the designated detection sites. Consequently, some microfluidic devices are designed to process only diluted whole blood samples to face this issue.

### Clogging

The risk of clogging within microfluidic channels increases with higher cellular content, primarily due to platelet aggregation and blood coagulation. To address this issue, dilution with a stabilizing buffer is commonly employed; however, this introduces an additional processing step and alters the original composition of the sample [30].

### Biocompatibility

Regarding biocompatibility, the primary challenge is selecting the appropriate material for a specific application while minimizing the risks of hemolysis, non-specific absorption, and platelet activation [30].

### Product Life Cycle

Most of the plasma separation devices are single-use and the life cycle of these products are not considered into account because of the contamination risks. Although some studies have been developed about biodegradable materials such polymers, this challenge remains, since polymer chips have a lower shelf-life compared to the traditional plastic chips [30].

### Physical Properties of Blood

In addition to the limitations mentioned before, the inherent physical properties of blood present significant challenges in the development of microfluidic devices for plasma separation. At large vessels, where shear rates are not high, blood assumes a Newtonian behavior and has a constant viscosity. On the other hand, in smaller vessels such venules and under low shear rates, blood is a non-Newtonian fluid, having features such shear-thinning viscosity and viscoelastic due to RBC aggregation and deformability.

Therefore, at low shear rates, RBCs form stacks of cells similar to coins (Figure 5a). These structures contribute to an increase in the bulk viscosity of blood, and consequently, can impede stable and uniform flows within the microchannels. However, at higher shear conditions, this aggregation is reversible and the RBCs elongate and align along the direction of flow. This characteristic behaviour of blood being dependent of different shear rates is a fundamental contributor to the viscoelastic nature of whole blood. Additionally, Fahraeus-Lindqvist effect, is another key phenomenon, which describes the reduction in apparent blood viscosity as microchannel diameter decreases. This behaviour results from the axial migration of RBCs toward the central region of the channel, where the flow velocity is highest. Consequently, the regions near the walls become depleted of RBCs, which results in the formation of a plasma-rich zone, known as the cell-free-layer (CFL) (Figure 5b). This formation presents lower viscosity compared to the central zone where RBCs are located, and is influenced by parameters such as hematocrit, RBC deformability and the channel geometry. Therefore, in the field of microfluidic device design, it is essential to study how flow resistance influences and enhances plasma separation.

In addition, plasma skimming is a phenomenon observed when bifurcation microchannels are used. This is characterized by the asymmetric distribution of RBCs during bifurcation, which consequently results in non-uniform hematocrit levels across branches. Usually, branches with lower flow rates or smaller diameters are more likely to receive plasma-rich streams with reduced hematocrit levels, due to axial migration of RBCs toward branches with higher flow rates. Thus, this behaviour can be advantageously used to enhance plasma separation. However, it also introduces an important consideration to be taken into account during the design of microfluidic approaches, because this phenomenon is influenced by channel geometry and flow conditions [33].

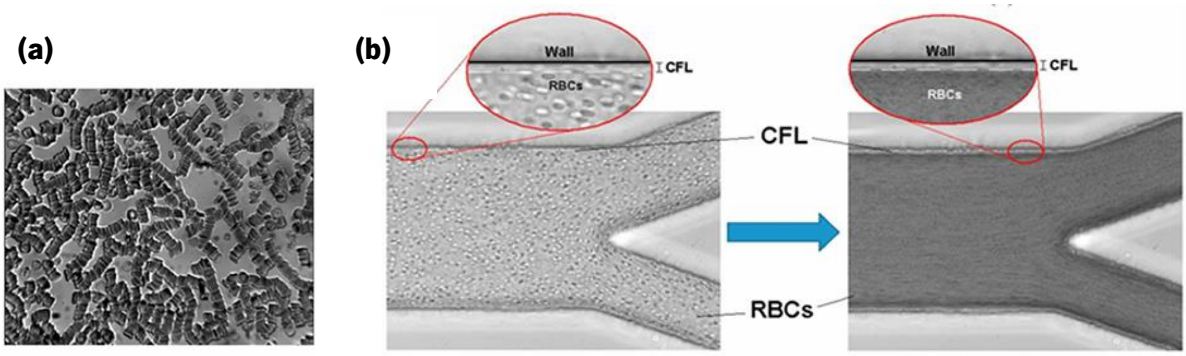



**Figure 5:** Different blood behaviours: (a) RBCs aggregation; (b) CFL region [33].

Beyond the discussion of the physical characteristics of blood that influence its microscale behaviour, it is equally important to study the performance of microfluidic devices for plasma separation based on critical operational parameters. Microfluidic devices for plasma separation are considered better when they achieve high purity, minimal hemolysis and a higher protein retention [2]. Therefore, before the introduction of blood-plasma separation techniques and their respective examples, it is essential to understand some lexicon of biological terms used at this field.

**Table 1:** Lexicon of terms used at the microfluidic field [30].

| | |
|---|---|
| **Dilution Ratio** | Ratio of the amount of blood compared to the total volume of sample after dilution. |
| **Extraction Rate** | Flow rate at which plasma reaches the outlet of the device during an experiment. |
| **Hematocrit** | Percentage of red blood cells in the blood. |
| **Purity** | Number of the RBCs remaining in the plasma that was extracted. Normally a percentage: $1 - \frac{cp}{cf}$. 100% purity indicates that no cells were detected in the plasma extracted. cp (number of RBCs in the plasma extracted); cf (number of RBCs in the plasma inserted). |
| **Yield** | Percentage of extracted plasma volume over the total volume of blood loaded. |

## 2.5 Blood-plasma separation techniques used in microfluidic chips

The limitations of macroscale centrifugation, the microfluidic's design challenges and the complex physical properties of blood mentioned previously have motivated the development of several microfluidic techniques in order to achieve an efficient blood-plasma separation at different conditions and configurations. Therefore, the following subchapter explores the theorical aspects of these techniques.
The miniaturized extraction of blood-plasma has been implemented in three main formats: microfluidic chip format, centrifugal disk (CD) format, and paper-based format. Paper-based format offers several advantages that make them attractive for PoC applications. These include low cost, portability [34], biocompatibility and flexibility [35]. In addition, their high porosity and transportation of fluid via capillarity action make them independent of external forces. However, limitation presented by this group are difficulties in manufacturing quality, precise fluid control and concerns regarding reagent stability and sensitivity over time. Furthermore, this technique presents difficulties in the integration with electronic devices [34], rapid coagulation and is limited to the analysis of highly concentrated analytes [30]. Challenges to pattern channels on paper are also faced [36]. In addition, in CD-like format systems the full integration, automation and miniaturization are possible [37]. On the other hand, abrupt changes in centrifugation frequency disrupt the system, causing premature reagent mixing or unintended dropet release. Furthermore, interference between different reaction steps can occur, specially in multi-stage detection processes, since centrifugal force enables parallel regulation [38]. Lastly, the movement of the fluid from one chamber to another depends only on the centrifugation [30].

Moreover, microfluidic chip format methods can be either passive [30] (advantage over cd-format) or active. In addition, compared to paper-based systems, these systems allow handling volumes and controlling flow with precision, are easier to integrate with electronics and when integrated have a low detection limit. Therefore, given these advantages for PoC applications, the microfluidic chip format was selected for plasma separation, being the chosen model explained at section 3.

As previously mentioned, two main categories of microfluidic techniques are employed at this format: active and passive methods [30]. The first group requires external forces [39], such external instrumentation or mechanical input by the user [1]. Other examples of external forces are the magnetic, acoustic and dielectrophoretic forces. On the other hand, the passive methods use properties of cells as a criterion to separate them, like shape, deformability and size. The separation is achieved also by varying the geometry of the microchannels, the natural flow and intrinsic hydrodynamic forces [30]. This approach does not require external instrumentation or even the mechanical stimulation by the user [1].

Some examples of passive techniques are filtration and sedimentation. In addition, deterministic lateral displacement (DLD) and the hemodynamic effect are other passive methods used to separate plasma from blood [40]. The following paragraphs will present theoretical background on active and passive methods. Figure 6 presents the classification of blood-plasma separation methods used in the microfluidic field.

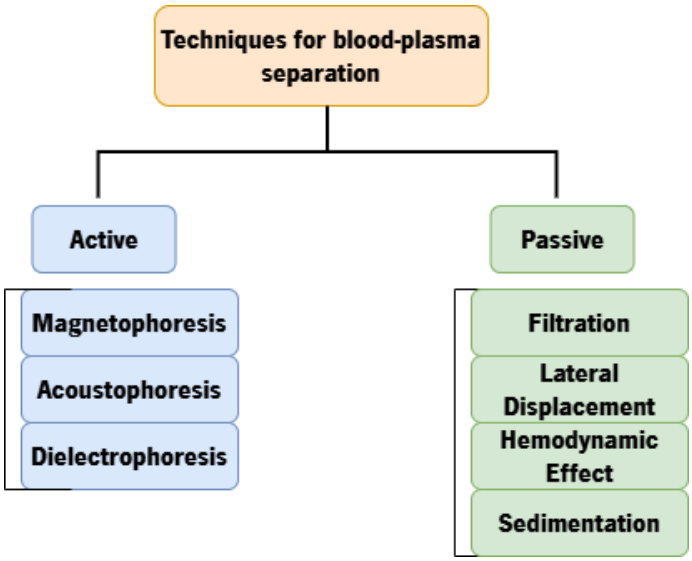



**Figure 6:** Blood-plasma separation techniques. Created with Biorender and inspired from [40].

### 2.5.1 Active techniques: theorical principles

The following paragraphs descrive the theoretical foundations of the methods that actively contribute for blood-plasma separation.

#### Magnetophoresis

Magnetophoresis has received attention around 2020 and preceding years, due to its relatively low cost and ease of implementation when compared to other active separation techniques [41]. It operates due to magnetic forces, being the particle's magnetic susceptibility (how easy the particle becomes magnetized), the non-uniformity of the magnetic field and the suspension medium, the main factors for the separation of bioparticles. Moreover, when magnetic susceptibility is positive, the material in question is classified as paramagnetic. Contrary, a material is categorized as diamagnetic when the susceptibility is negative. Besides, when a paramagnetic particle experiences attraction toward the magnetic field, this

process is called positive magnetophoresis, while negative magnetophoresis is known for the opposite behaviour, when a diamagnetic material is exposed to a magnetic field [42], [43]. Figure 7 represents magnetophoresis from a particle perspective in a non-uniform magnetic field. It illustrates two magnets, each one with two poles (S, south and N, north), with the magnetic flux density increasing from left to right. As referred before, since the red particle is paramagnetic (positive $X_p$) and the medium is diamagnetic (negative $X_f$), the red particle will experience attraction toward the magnetic field (represented as $F_{pMAG}$- blue vector, positive magnetophoresis). On the other hand the yellow particle is diamagnetic (negative $X_p$) and the medium is paramagnetic (positive $X_f$), the yellow particle will be repelled toward the opposite direction (represented as $F_{nMAG}$- red vector,negative magnetophoresis).

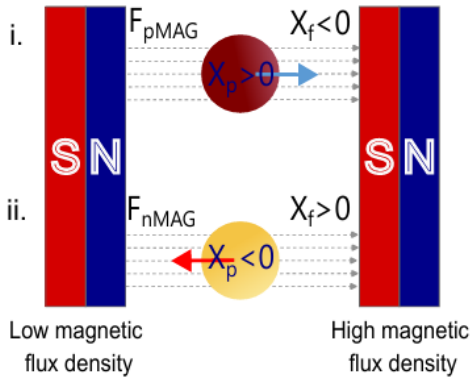



**Figure 7:** Illustration of magnetophoresis. It illustrates the displacement of particles either toward the magnetic field (indicated by the blue vector) or away from it (indicated by the red vector). This movement is governed by the difference in magnetic susceptibility between the particle ($\boldsymbol{X_p}$) and the surrounding medium ($\boldsymbol{X_f}$) [42].

Magnetophoresis requires magnetic particles. However, most of the particles encountered do not have magnetic properties. This limitation is addressed by magnetically labelling the target particles with magnetic beads (micro- or nanoscale particles). Figure 8 shows a schematic of magnetophoresis technique where the target is labelled with magnetic beads [43].

In microfluidic systems which employ magnetophoresis, magnetic forces enable the transport, separation, immobilization and sorting of magnetizable and non-magnetizable particles.

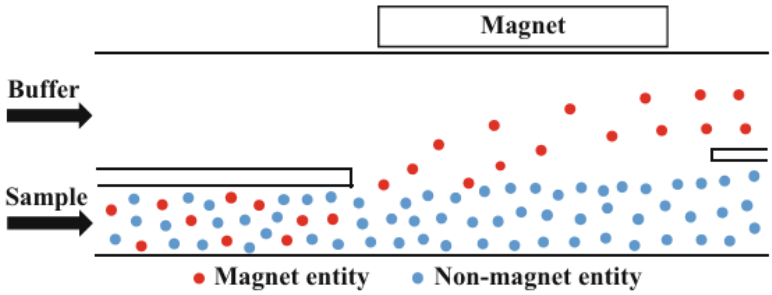



**Figure 8:** Illustration of magnetophoresis with labelled target with magnetic beads [43].

The immobilization method is usually applied in batch-type scenarios. Additionally, transportation is accomplished by pulling the fluid and the particles with a directional magnetophoretic force or by dragging the particle with a carrier fluid or in pressure driven mode.

Furthermore, the magnetic separation is divided into two groups: trapping (capture)-based or continuous-flow based. In the first group, magnetically labelled particles are introduced into a microchannel under pressure-driven flow and are trapped at capture sites due to localized magnetic fields. Once immobilized, reagents can be introduced over the particles to enable surface-based biochemical reactions. Following this step, the particles may be retained, washed or released for analysis [43]. Figure 9 exhibits a magnetophoretic capture-based example.

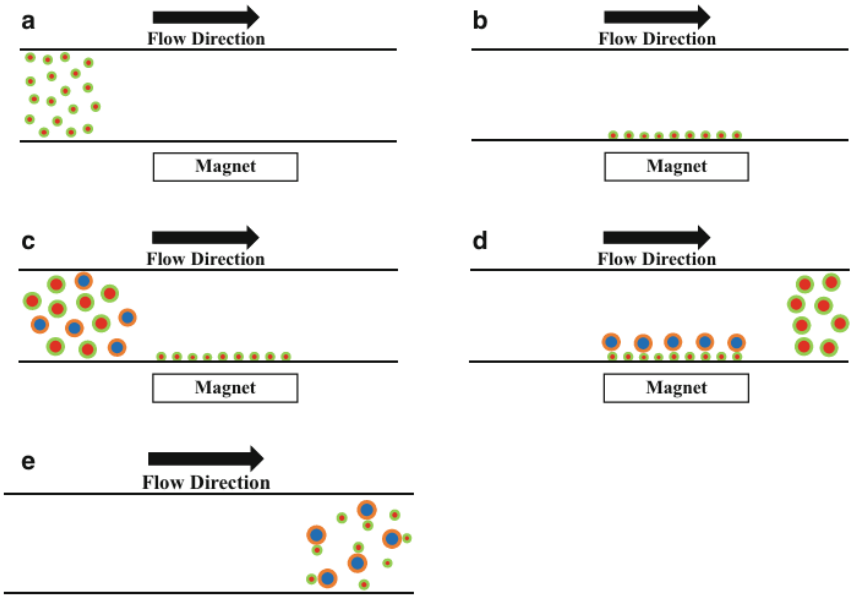



**Figure 9:** Illustration of capture-based separation: (a) Introduction of magnetic beads; (b) Trapping magnetic beads with a magnet; (c) Introduction of a sample containing target cells; (d) The target cells are captured; (e) The magnet is removed to release the target population of cells [43].

Capture-based separation has inherent limitations, such as its discontinuous operation and the requirement for multiple sequential steps. In contrast, continuous-flow magnetophoresis-based separation allows for the deflection of particle trajectories across the width of the main channel toward designated outlets, depending on the orientation of the applied magnetic field, which can be perpendicular or oblique to the laminar flow (Figure 10). A key advantage of this approach is its ability to process samples continuously, without constraints related to sample volume or processing time [43].

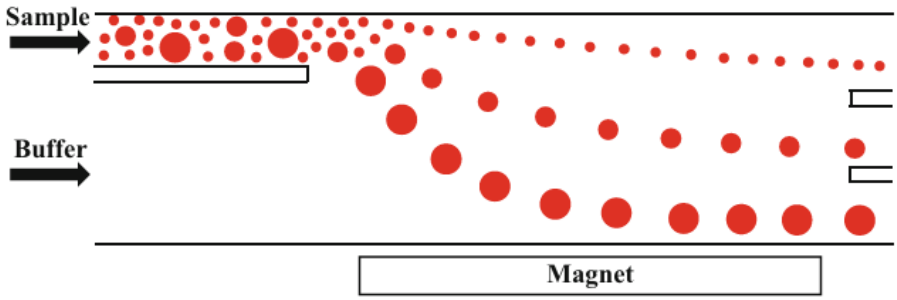



**Figure 10:** Illustration of continuous-flow magnetophoresis [43].

### Acoustophorsesis

Acoustophoresis uses acoustic waves that interact with a medium, in order to separate, trap or sort its particles such as blood cells [42]. A major advantage of this method lies in its noninvasive nature, enabling label-free manipulation of particles [43]. Additionally, in this technique, acoustic waves are formed by a resonant device near or within microchannels, being for example transducers on piezoelectric substrates or thin films [42]. When subjected to an electric field, the transducer generates mechanical vibrations that, in turn, induce the movement of particles. A schematic representation of acoustophoresis is shown in Figure 11.

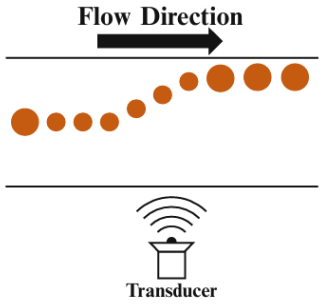



**Figure 11:** Illustration of acoustophoresis [43].

The acoustic contrast factor determines the direction of particle migration within an acoustic field, whether a particle will be driven toward a pressure node (positive contrast) or toward an anti-node (negative contrast). The sign of this parameter, and consequently the direction of the particle migration is dependent of the comparative density and compressibility of the particles and its surrounding medium [43]. Normally, gaseous particles, show a negative contrast factor and are directed toward pressure anti-nodes. Contrary, solid particles such cells, tend to move toward pressure nodes, exhibiting a positive contrast factor [42]. Figure 12 illustrates the behaviour exhibited by a heterogeneous suspension at a microchannel, when exposed to an acoustic wave. This acoustic field establishes a central pressure node and pressure antinodes at the sidewalls. Given that the red particles possess a positive acoustic contrast factor and the green particles a negative one, the two populations undergo distinct manipulations under the acoustic field. Thus, while green particles are moved toward the sidewall antinodes, the red particles are acoustically focused toward the central node, aligning along the vertical midline (Figure 12c).

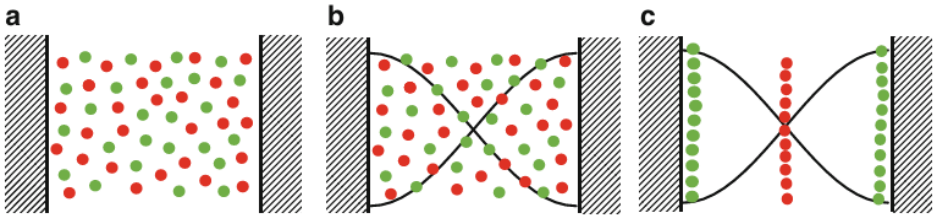



**Figure 12:** Illustration of the separation of a heterogeneous sample via acoustophoresis: (a) Heterogeneous sample (red and green particles); (b) The sample is exposed to an acoustic field; (c) Due to acoustic contrat factor, red and green particles move toward different positions; Green particles are moved toward the sidewall antinodes and the red particles move toward the central node [43].

### Dielectrophoresis

Dielectrophoresis (DEP) consists in the application of DC and AC voltage in a microfluidic channel, generating a non-uniform electrical field, which results by varying the geometry or the shape of the microfluidic channel. This technique is rapid, non-invasive and highly selective and sensitive [43]. When the electric field interacts with the medium and the particles in question, a polarization effect occurs, characterized by the electrical difference between the electrical properties of the sample compared to the medium. Consequently, this response can be either the movement of the particle towards (positive DEP, pDEP) or away (negative DEP, nDEP) from zones of higher electric field, if the particle polarizes more or

less than surrounding medium, respectively [42]. Figure 13 shows the movement of particles due to negative and positive DEP forces.

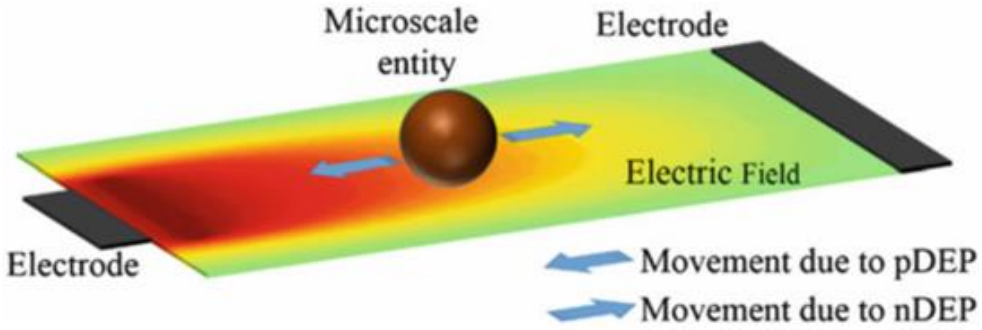



**Figure 13:** Illustration of dielectrophoresis [43].

DEP separations can be divided into multistep and continuous separation platforms. Subsequently, the first category can be achieved by DEP retention and DEP migration.

On the other hand, DEP deflection is included in the continuous separation [43]. DEP retention is applied to retard the motion of the particles in the microchannel, by applying a positive dielectrophoretic force (pDEP). When the dielectrophoretic force and hydrodynamic drag force are balanced and the resultant force approaches zero, the particle immobilization is achieved. At the same time, the remaining particles that experience negative DEP or a weaker pDEP continue to travel along the microchannel, remaining the drag force, the dominant one. On the other hand, the DEP migration technique consists in the collection of targeted particles at certain locations through the microchannels, by applying DEP forces, both pDEP and nDEP. In addition, the particles are collected in a subsequent step. Furthermore, in the continuous DEP deflection method, the non-target particles follow the main fluid stream, exiting from different outlets, while the target microparticles are directed toward a specific outlet. Figure 14 illustrates the schematic representation of DEP-based separation by retention (Figure 14a), migration (Figure 14b) and deflection (Figure 14c).

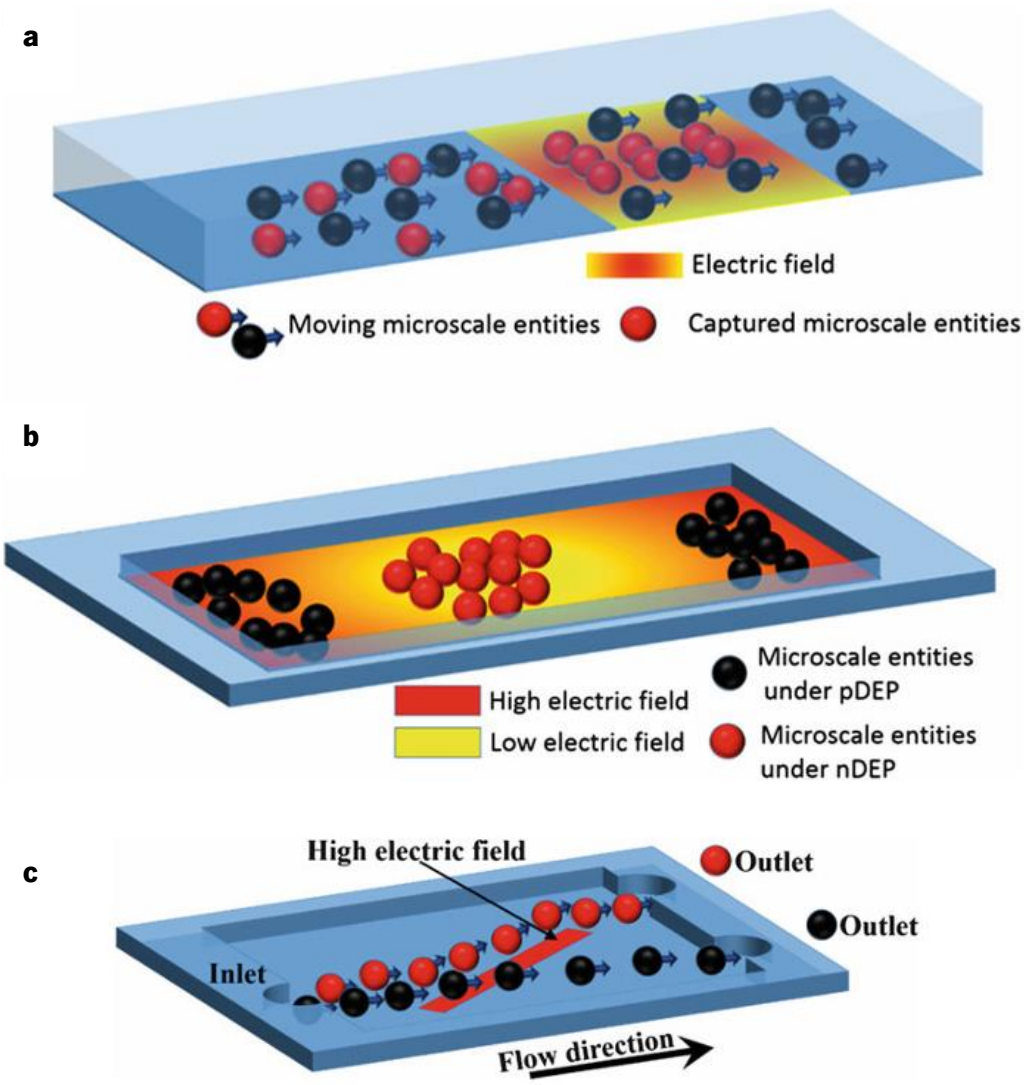



**Figure 14:** Multistep and continuous DEP: (a) Retention; (b) Migration; (c) Deflection [43].

### 2.5.2 Passive techniques: theorical principles

The subsequent paragraphs discuss the fundamental concepts of the passive technqiues applied in blood-plasma separation.

#### Filtration

Filtration is an example of macroscale technique of blood separation that has been miniaturized (microfiltration). This technique is based on particle size differences and the segregation by dimensioned pores [30]. Micropillar arrays or microporous membranes are some examples used to separate cells and particles based on their density, shape and deformability [44]. Additionally, filtration is divided in dead-

end microfiltration and cross-flow microfiltration. While in the first variety, the blood flows perpendicular to the filter, in the second type, the blood separation occurs tangentially to flow direction [30] (Figure 15).

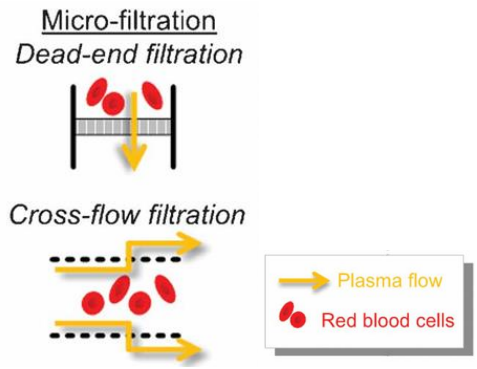



**Figure 15:** Illustration of dead-end and cross-flow filtration. Edited from Figure 3 from [30].

### Sedimentation

Sedimentation is based on the difference between plasma density and blood cells. It is often combined with other techniques such as filtration, since the rate of blood cells sedimentation is low and the separation of plasma consumes a considerable amount of time [45]. Figure 16 presents an illustration of this method.

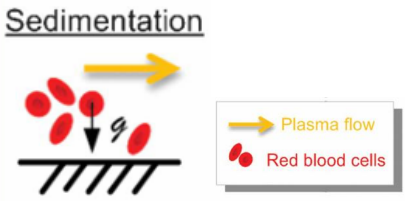



**Figure 16:** Illustration of sedimentation-based technique for plasma separation. Edited from Figure 3 in [30].

### Lateral displacement

Lateral displacement uses an array of pillars, in which the distance between them is chosen depending on the cell size to be separated. The fluid flows in a laminar manner, interacting with the array of pillars, which consequently guide the cells along specific paths. In this technique, cells with different sizes behave in distinct ways. Particles with diameters smaller than the array gaps pass through the gaps and remain close to the original central streamline. Contrary, the cells larger than the array gap tend to

flow laterally and at an angle determined by the post offset distance [44]. This approach has emerged as a prominent method in microfluidic systems, due to its operational simplicity and high precision [46]. Figure 17 presents the displacement exhibit from small and large particles in the lateral displacement method.

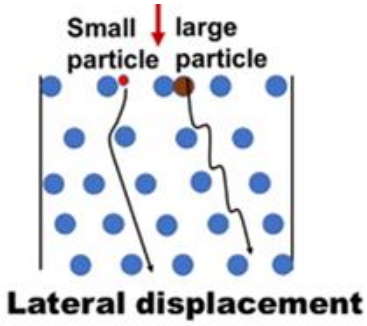



**Figure 17:** Illustration of the lateral displacement technique. Edited from Figure 2 in [40].

### Hemodynamic phenomena

Several hemodynamic phenomena observed *in vivo* have also been translated to microfluidic devices. Among these phenomena are the Fahraeus–Lindqvist effect, which refers to the migration of red blood cells (RBCs) toward the center of the channel, resulting in the formation of a cell-free layer (CFL) near the channel walls, as previously mentioned; leukocyte margination, which is defined as the movement of leukocytes, which are less deformable than RBCs, toward the channel walls due to collisions with RBCs; plasma skimming, which describes the unequal distribution of RBCs and plasma between the main channel and a branching side channel, as noted earlier; and the Zweifach–Fung effect, also known as the bifurcation law, in which the branch with a lower flow rate receives a relatively higher proportion of plasma [44], while the volume fraction of RBCs increases in the branch with the higher flow rate [47]. Figure 18 presents a schematic of hemodynamic effect, specifically the bifurcation law.

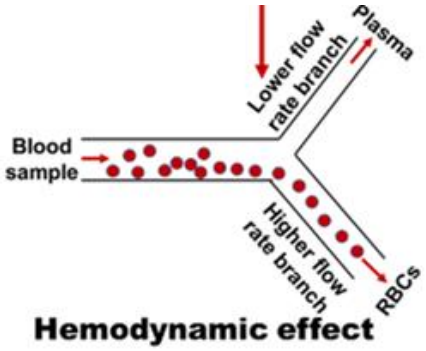



**Figure 18:** Illustration of hemodynamic effect- Bifurcation Law. Adapted from Figure 2 in [40].

In general, passive techniques offer severable benefits such operational simplicity, low cost and minimal instrumentation requirements. Although, some limitations presented by this group of techniques are separation precision and efficiency, extended processing times or larger sample volumes to achieve satisfactory results. Conversely, active separation methods offer enhanced precision and high efficiency. However, these type of methods require specialized equipment, which can increase the cost of implementation and the complexity of the system [48]. In other cases, hybrid methods are also applied. These techniques combine active and passive methods, leveraging their combined strengths [49].

### 2.5.3 Representative studies on active microfluidic techniques for blood-plasma separation

In this subchapter, published studies on active plasma separation techniques will be discussed, including magnetophoresis, acoustophoresis and dielectrophoresis.

#### Magnetophoresis

*Kwon et al.* developed a polydimethylsiloxane (PDMS) diamagnetic blood-plasma separation from undiluted whole blood device (Figure 19ai). In previous studies, this team concluded that adding superparamagnetic iron oxide nanoparticles (SPION) to whole blood would increase the magnetic susceptibility of plasma. Consequently, under a magnetic field, the blood cells would be repelled with forces, strong enough to separate them from plasma. Therefore, a permanent magnet (Halbach magnet array) was placed adjacent to the microchannel to create a gradient in magnetic flux density. In addition, the device consisted of an inlet for insert whole blood and two outlets, one to repel blood cells and the

other to separate plasma, where syringe pumps were connected to apply negative pressure and move the sample within the channels.

Additionally, iron oxide microparticles were added into the plasma's channel and generated higher magnetic forces that removed SPIONs from plasma (Figure 19aii). This action was necessary to remove SPION's interference in specific applications, such as molecular diagnostics. This method achieved 100% plasma purity and a plasma yield of 83.3%. Therefore, the plasma approach developed offered a combination of advantages: enabled the isolation of plasma from whole blood without dilution, achieved 100% purity and minimized the risk of shear stress-induced hemolysis. In samples processed through the device, it showed a strong linear correlation between prostatic specific antigen PSA concentration and the intensity of fluorescence, matching the performance of traditional ELISA with centrifuged plasma. The approach achieved a limit of detection (LOD) of 2.5 ng/mL, which is a successful result, due to the diagnostic threshold for PSA (4 ng/mL). Furthermore, it demonstrated a clinical advantage in preserving and recovering biomolecular targets such as bacterial deoxyribonucleic acid (DNA), which is usually lost during centrifugation. To conclude, these findings showed the capacity of the device to function on PoC applications and immunoassays without centrifugation [50].

*Zeng et al.* introduced a cost-effective power-free device for plasma separation based on negative magnetophoresis for later biochemical analysis (Figure 19bi). This system used a ferrofluid, a colloidal suspension of magnetic particles, mixed with whole blood. The ferrofluid created a concentration gradient due to its attraction to areas with high magnetic field. Consequently, this gradient formed a region near the magnet of concentrated magnetic fluid and a lower concentration far away. As a result, blood cells, characterized by being non-magnetic particles, were repelled from the magnet (negative magnetophoresis). While larger blood cells were repelled to the centerline of the channel, plasma accumulated on both sides of the channel close to the magnet array. The system consisted in a double Halbach magnetic array with different sizes arranged alternately and a throughput-adjustable separation channel integrated, allowing modifications to its height (H) and length (L) while maintaining a fixed width. Whole blood went to the separation section, through gravity, existing at the end of the channel's exit, a double-layer chip to separate plasma from whole blood (Figure 19bii). Regarding to the key findings, the team determined that the system can handle whole blood volumes ranging from 100 μL (of rat blood) to 3 mL (of human blood) per cycle, through adjusting the channel height. In addition, the separation time was dependent on the blood type and viscosity, achieving 3mL of plasma in 1 min from a sample of human whole blood and 40 μL of plasma in 8 min from 100 μL of rat whole blood.

The team of researchers also concluded that in the experiment with rat blood, the plasma extracted for antibody drug metabolism analysis showed particle size and concentration similar to the plasma obtained via centrifugation. On the other hand, in the experiment with human blood, the ELISA test detected with success the target in question. In both tests (human and rat blood samples), the system achieved 99.9% of cell separation efficiency, for cells larger than 1 μm, and the plasma rate reached 72.7%, demonstrating that the system provides a high yield compared to traditional methods. To conclude, this approach enabled manual operation and was considered suitable for PoC testing and remote and resource-limited locations. The device had also a high-throughput capability and facilitated rapid plasma extraction from whole blood [51].

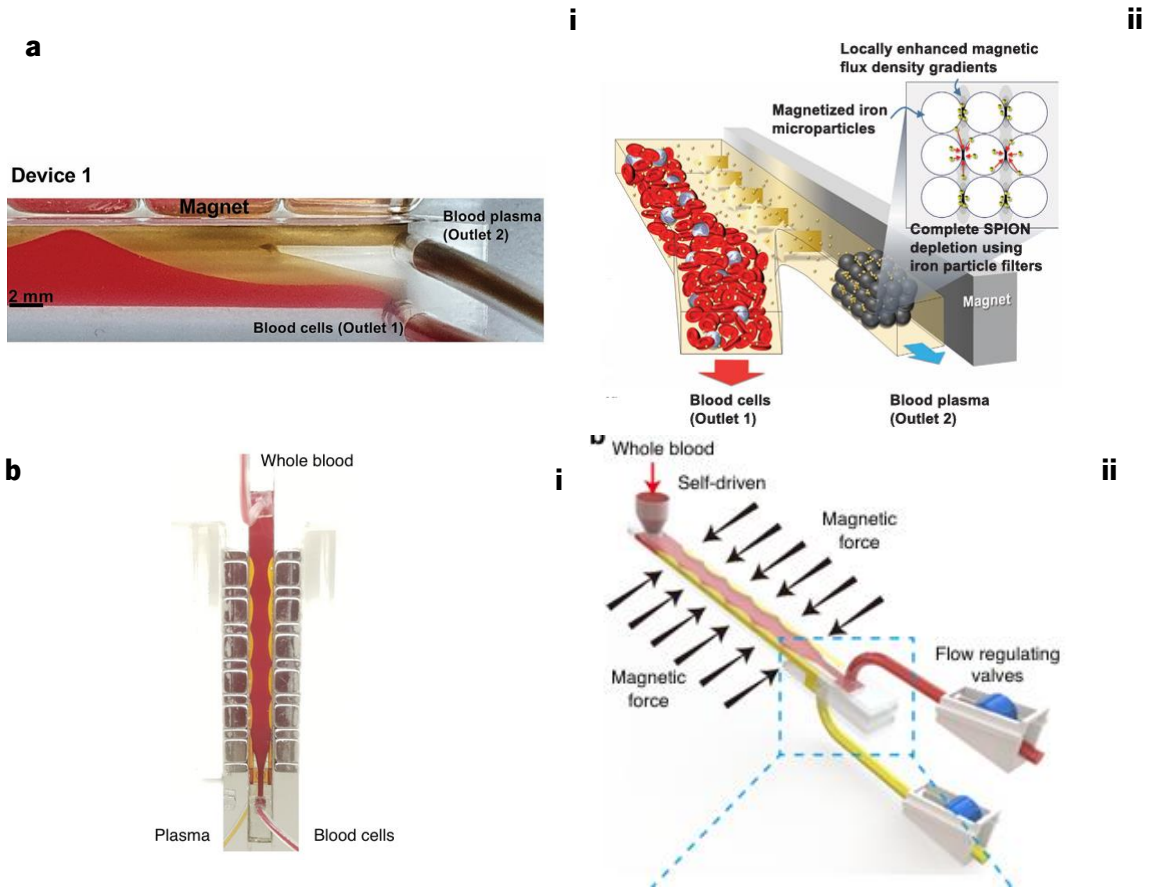



**Figure 19:** (a) Diamagnetic blood-plasma separation from undiluted whole blood device using SPIONs: (i) Cross section of the system and (ii) Schematic of the device [50]; (b) Power-free device for plasma separation based on negative magnetophoresis: (i) Visual representation of the experimental setup and (ii) Schematic diagram of the system. Adapted from [51].

**Acoustophoresis**

An alternative microfluidic apparatus was designed by *Liu et al.* , integrating several functions on a single chip and using the principle of bubble-induced acoustic microstreaming to test whole blood controls spiked with fluorescently tagged antibodies to HIV-1 p24 protein. (Figure 20ai). Here, a piezoelectric ceramic (PZT) transducer created an acoustic field that acts at an air bubble. The vibration of the PZT made the air bubble oscillate, creating microstreaming vortexs and, at a specific frequency, this method had the ability of trapping blood cells inside the microstreaming vortex (Figure 20aii). In addition, the behaviour of the particles within the microstreaming vortex was determined by their size and density. While smaller particles, as RBCs, occupied larger orbits, tighter orbits were occupied by greater blood cells such as WBCs. Simultaneously, plasma elements travelled downstream because they did not occupy any orbits due to their smaller size compared to the blood cells (Figure 20aiii). In addition, along the microchannel, the further sections had fewer blood cells compared to the initial ones and after several turns in the serpentine channel with diverse cavities to trap blood cells, a pure plasma solution was produced with this device (Figure 20aiv). At the end of the plasma separation channel, the separated plasma was mixed with HIV-1 p24 antigen conjugated beads in an integrated micro-mixing chamber. Acoustic microstreaming subsequently enabled the capture of p24 antigen–antibody complexes, which were detected using a fluorescence microscope. As a result, the presence of the p24 antigen was successfully identified. The detection limit of the device was demonstrated to be ∼17 pg/μL, indicating that several functions can potentially be combined with acoustic microstreaming on a single microfluidic approach, allowing the detection of a specific biomarker. With this device, about 15.9 μL of plasma was separated from undiluted 50 μL of blood sample. In addition, it was obtained 99.9% of plasma purity and 31.8% of plasma yield, being this value lower compared to 55% of centrifugation's plasma yield, but greater than other similar devices. Finally, acoustic microstreaming offered several advantages over other plasma separation methods, including a simpler device design, easier operation and fabrication, and reduced risk of clogging due to the large width of the microchannel [52].

*Ma et al.* developed an impedance mismatch-assisted, titled-angle acoustofluidic separation technology (Figure 20bi). This system separated plasma from blood cells through acoustic forces generated by piezoelectric transducers, which were attached to the sides of the device. When the transducers were activated, acoustic waves were generated, forming multiple pressure nodes inside the microchannel. Consequently, these pressure nodes were positioned depending on the difference in acoustic impedance between the channel walls (made of polymethylmetacrylate, PMMA) and the blood medium (phosphate buffered saline, PBS). Regarding the separation mechanism, without an acoustic

signal, blood entered in the microchannel and the components moved toward the lower outlet (Figure 20bii, left side). Although, when the piezoelectric transducers were working, the acoustic waves flew at different speeds between PMMA and PBS, leading to refraction at the liquid-solid interface, contributing to the titled-angle acoustic pressure distribution field. Blood cells experienced the acoustic radiation forces in diverse ways, depending on size differences. Since RBCs and WBCs were larger than platelets and plasma proteins, they were subjected to higher acoustic forces. Consequently, when the fluid that filled the microchannel was homogenous (it had only one fluid), the cells experienced solely the acoustic force. Therefore, RBCs and WBCs moved to the upper outlet, while platelets moved to the lower outlet, along with plasma proteins. However, when a sheath fluid such as PBS was introduced alongside whole blood within the microchannel, the resulting mixture formed an inhomogeneous fluid. Thus, a mismatch in the acoustic impedances between whole blood and the conventional sheath flow was introduced, creating an additional driving force. Consequently, when the piezoelectric transducers worked, it was possible to achieve the separation of the platelets driving them to the upper outlet along with RBCs and WBCs, allowing the separation of plasma from blood cell (Figure 20bii, right side). Finally, the team of researchers concluded that this mechanism achieved an efficient removal rate of RBCs, WBCs and platelets of 85-95% and a throughput of 20 μL/min. In addition, by altering the voltage and sample flow rate within a range of 21-27 voltage peak to peak (Vpp) and 10-25 μL/min, it was possible to regulate the efficiency of blood-plasma separation. To conclude, this device was suitable for plasma-based separation and further biomarker analysis, owing to its high biocompatibility, label-free nature, cost-effectiveness, and automated processing capabilities [53].

**Dielectrophoresis**

*Chen et al.* developed a capillary-driven, portable and contactless dielectrophoresis (cDEP) microfluidic chip that uses low voltage of ~1V to separate plasma from an undiluted blood sample (Figure 21a). Regarding the working principle, when whole blood samples were introduced into the chip, the blood flew quickly because of the capillary action that arises from the hydrophilic behaviour of the glass presented at the channel walls. Red blood cells and plasma travelled at the same speed, at this point (Figure 21b). When an AC voltage was applied, the asymmetric shape of the electrodes produced an inhomogeneous electric field. RBCs became polarized and interacted with it, leading to their aggregation (Figure 21c) [54].

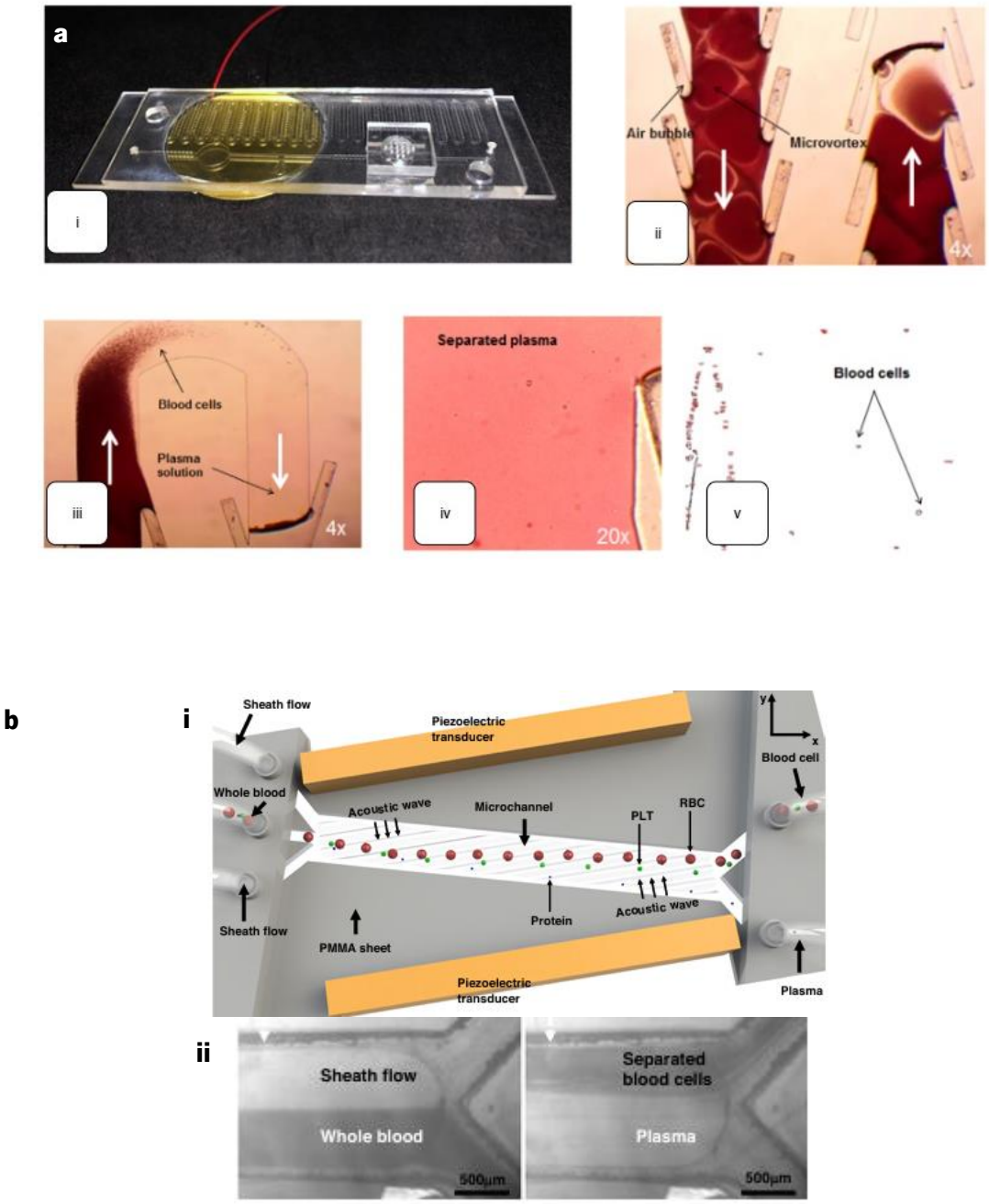



**Figure 20:** (a) Microfluidic for blood-plasma separation and detection of biomarkers using acoustic microstreaming: (i) Design of the system and (ii) Images demonstrating the plasma separation at different locations of the device. Adapted and edited from [52]; (b) Impedance mismatch-assisted acoustofluidic device: (i) Schematic of the system; (ii) Left, acoustic transducer off: whole blood is collected at the lower outlet. Right, transducer on:blood cells are separated to the upper outlet, when a sheath fluid is introduced [53].

The velocity of the RBCs decreased when the dipole-dipole interactions became strong enough to overcome the capillary force. Simultaneously, once the plasma was not affected by the electric field, it kept moving forward due to capillary forces (Figure 21d). Therefore, this difference in velocity was the primary factor responsible for the separation of plasma from whole blood. In addition, the team studied two experimental variables such the frequency of AC voltage and the Vpp. They applied AC voltages with frequency ranging from 100 kHz to 10 MHz, and found that higher frequencies led to stronger cell interactions and faster plasma separations. Contrary, at 100 kHz and 1 Vpp, the team did not achieve plasma separation because the low frequency may be blocked by cell membranes and only a small dipole-dipole interactions occur between cells at this frequency. Additionally, researchers studied the effects of the voltage, ranging from 1 Vpp to 3 Vpp at a constant frequency of 1 MHz. They concluded that 1 Vpp was effective to separate plasma from whole blood and higher voltages led to a better RBC aggregation and reduced separation time due to the enhanced strength in the electric field. Furthermore, due to the low voltages application, and the absence of contact between electrodes and the samples, the formation of bubbles and the heat production was avoided. More importantly, the hemolysis effect was not noted. To conclude, this microfluidic approach achieved a separation efficiency and a separation quality of 69.8% and 89.4%. respectively, within a reasonable separation time [54].

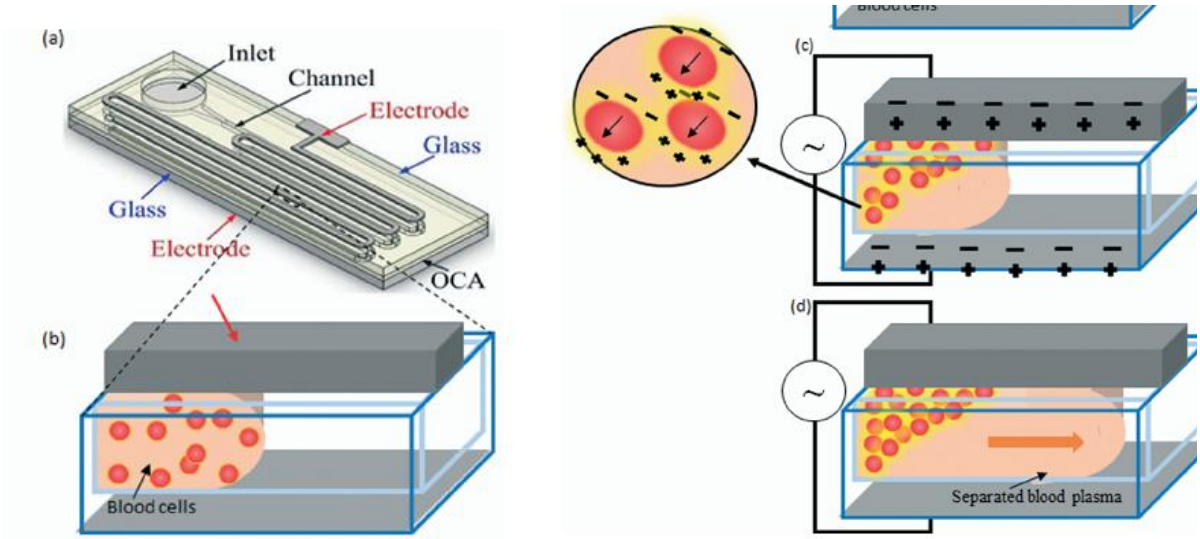



**Figure 21:** Dielectrophoretic microfluidic chip for plasma separation: (a) Schematic of the system; (b) RBCs are dispersed when the voltage is off; (c) Voltage on:Positive DEP drives RBCs to the surface; (d) While plasma flows over time, RBCs remain aggregate. Adapted from [54].

### 2.5.4 Representative studies on passive microfluidic techniques for blood-plasma separation

Devices employing passive techniques have been also developed, being presented in this subchapter.

#### Filtration

*Zhang et al.* presented a blood-plasma separation system in PDMS with crossflow microchannels that use size exclusion cell separation as principle. Three ports made up the device, an inlet for the whole blood sample and two outlets, one for the separated blood and the other for the separated plasma. In addition, crossflow channels were positioned between the plasma channel and the whole blood channel (Figure 22ai). Regarding the functionalization, due to the crossflow channels mentioned before, the plasma flew out from the blood channel to the plasma channel, being separated from the whole blood. At the same time, the blood channel continued to transport blood cells and unseparated blood-plasma until the separated blood outlet. In traditional crossflow techniques, the crossflow microchannels are placed in a linear format, where the plasma channel widths at the inlet and outlet as well as the crossflow channel widths are the same, contrary to this device. Here, the microchannels were placed into a circular arrangement (Figure 22aii). The new circular configuration used minimised the device's footprint for PoC diagnostics and created an exterior radial force that helped minimising hemolysis, once the contact between the RBC's and the crossflow microchannel was decreased. In addition, the likelihood of cells obstructing the microchannels was reduced, which contributed to an overall improvement in plasma separation efficiency. Furthermore, the RBC leakage into the plasma channel was reduced and the blood-plasma separation throughput was increased. To achieve this objective, the crossflow channel was progressively widened in the high-pressure regions near the inlet and further downstream, respectively, as illustrated in Figure 22aii, where T4 is greater than T3. Simultaneously, the plasma channel was progressively widened (W3 < W4) as shown in the same figure, which increased flow resistance and consequently reduced the pressure at the interface between the blood channel and the plasma channel near the inlet. This pressure drop helped prevent the entry of red blood cells into the plasma channel. This improved the separation efficiency and the collection of plasma along the channel. Finally, the crossflow channels were positioned at the bottom of the blood channel, enhancing the Fahraeus effect at the corners and reducing the concentration of blood cells. These modifications enabled a plasma extraction yield of 22% and a red blood cell separation efficiency of 97% from 50 µL plasma samples,

with hemolysis levels ranging from 0.01% to 0.5%. In addition, less RBC clogging was reached with this new approach. Furthermore, conventional crossflow methods struggle to achieve high separation efficiency with a low degree of hemolysis, being the dilution or slower flow rates the solutions used to face this challenge. However, such method is inappropriate for PoC. On the other hand, with this new approach no blood sample's dilution was achieved. To conclude, compared to the conventional linear arrangement, the circular configuration demonstrated benefits regarding the recovery rate, the level of hemolysis and the reduced RBC clogging. Finally, this compact and passive system, which produces high-quality plasma, can be applied in a variety of PoC applications involving blood biomarkers [31].

*Brakewood el al.* engineered a device capable of separate plasma from whole blood, using depth filtration as separation method and capillarity action as plasma's collection process (Figure 22b). Device properties such the channel width, collection mechanism and the input volume were optimized for a better output volume yield and plasma quality. This device does not need the use of external and complex equipment. More specifically, this approach used a plasma separation filter that was integrated with a microchannel on a double-sided adhesive. During the fabrication, a 60 x 60 mm adhesive was cut, along with an inlet well, an outlet well, and a channel connecting the two wells. Additionally, a glass coverslip was added to the top of the adhesive to form the main channel, without covering the inlet well (Figure 22bi). To form the collection area at the outlet well, a second adhesive was inserted there (Figure 22bi). On the other hand, at the inlet well, a filtration membrane was placed (Figure 22bi). Thus, the sample was pipetted on the filter, which traps the RBCs by using an agglutinating chemical retention of 4 μm. Contrary, the plasma was able to pass in the filter via gravity. After it, plasma passed through capillarity from the inlet well through the channel, into the collection area, from which it was collected using a pipette. With an input of 50-100 μL of whole blood sample, the production of plasma can occur in less than 2 min. More specifically, a maximum of 14 μL of plasma was obtained from 50 μL of whole blood, corresponding to a maximum separation efficiency of 88.5%. Due to its cheaper way of manufacturing and easy operation, this microfluidic device is suitable for PoC applications. However, this new device has some limitations, including the production of samples with RBC contamination and requires a minimal sample size in the range of tens of microliters, being a limitation for diagnostic applications of the device [29].

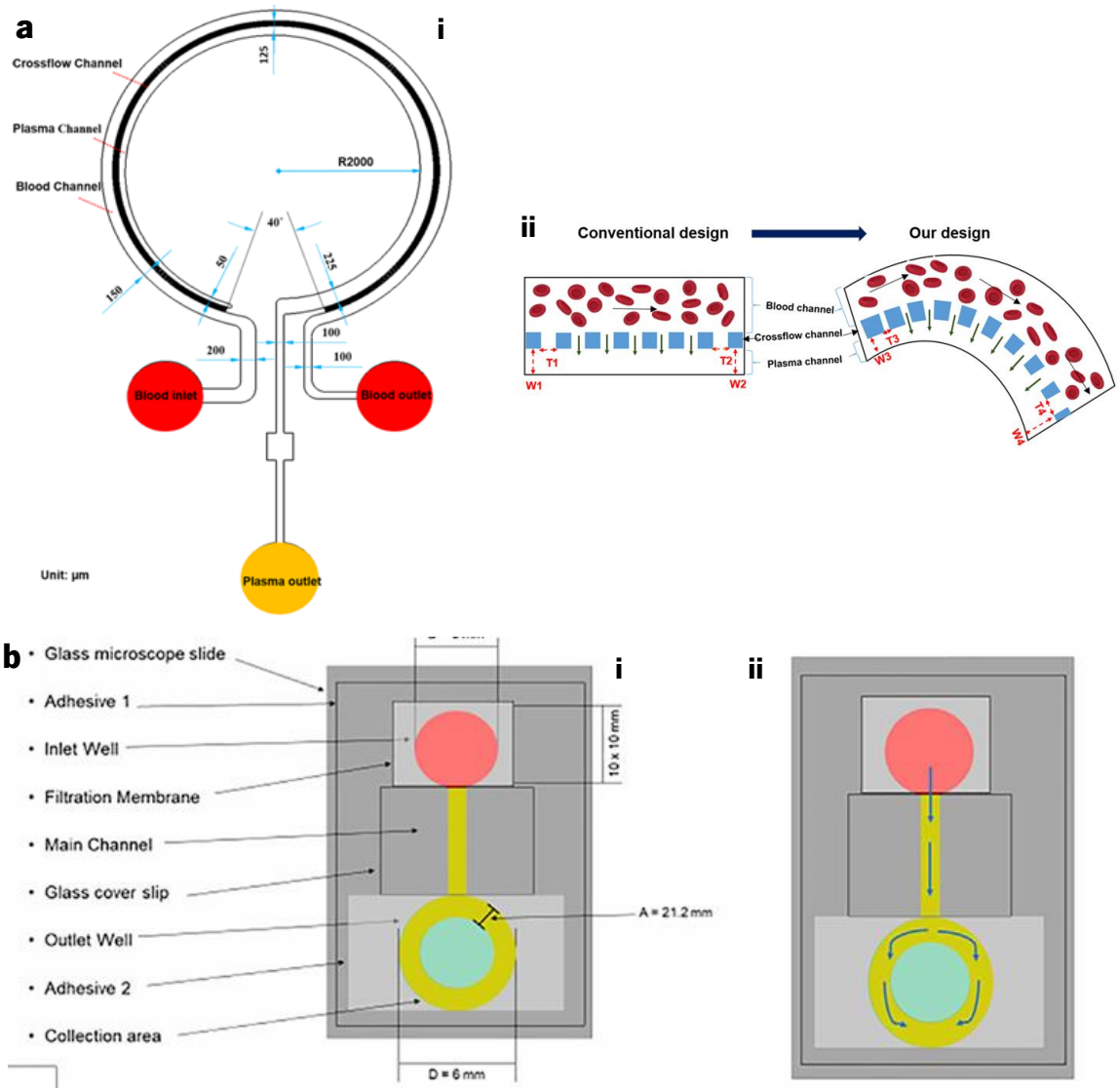



**Figure 22:** (a) Circular gradient-width crossflow plasma separation device: (i) Top view; (ii) Comparison of traditional straight crossflow vs. new developed curved, gradient-width crossflow design [31]; (b) Filtration-based microfluidic chip: (i) Adhesive was cut to include an inlet well, outlet well, and a channel connecting them and filtration membrane placed over inlet well. Whole blood (red) is applied onto the filter; (ii) Plasma path indicated by arrows. Adapted from [29].

## Sedimentation

*Debnath et al.* developed a new technology with two elements integrated: a device which separates plasma from a whole blood sample, without external forces and a surface plasmon resonance (SPR) sensor to detect biomarkers in plasma (Figure 23a, left side). The separation device, referred to as PPS-V2 (Figure 23a, right side), is an enhanced version of the original device (PPS, version 1) and uses a pipette/syringe-based sample collection method The device comprises three PDMS layers with

microcapillaries (PDMS layers 1, 2 and 3) and a thick membrane between the middle layer and the top layer (Figure 23b). The blood moves through the capillary microchannel that exists at the PDMS layer 1, from the inlet well to the end of the capillary. Furthermore, an entrance well (W1) for loading the blood sample and an exit well (W2) that establishes a connection to the top fluidic microchannels, are included in the PDMS layer 2. The PDMS layer 3 is composed by the capillary micropump for plasma collection and some plasma outlet reservoirs (Figure 23c). Additionally, due to the presence of a built-in filter, W2 serves as the site of plasma separation, which results from the wettability gradient established in that region. In addition, the thick membrane previously referred located between the middle and top layer, allows the removal of blood cells. It takes 1 min for the blood to reach the bottom capillary as the inlet is filled with 80-200 µL of whole blood sample. Subsequently, plasma separation occurs at PDMS layer 2 through sedimentation and the wettability gradient, a process that takes approximately 10 min. In the end, only plasma with a lower amount of blood cells passes to the top microchannels, being indicative of the self-built-in filter formation mentioned before. This device achieves approximately 86% purity and a yield of around 25%, allowing the collection of 22 µL of plasma from 160 µL of whole blood within 15 min. In conclusion, the whole blood samples used required no pre-processing, and the developed device demonstrated portability and ease of fabrication. [55].

**Hemodynamic Phenomena**

Abouali *et al.* from the University of Waterloo have designed three hydrodynamic continuous, high-throughput plasma separator (HCHTPS) microfluidic devices through computational and experimental assessments. The HCHTPS microfluidic devices contain a main channel in expanded and contracted parts. In addition, the main channel has sixteen channel expansion areas (CEAs) and asymmetrical parallel side channels with variable lengths, same width and height, placed at the corner of the first twelve CEAs for plasma drainage (Figure 24a). From previous studies, the team decided to vary the length to maintain a constant extraction rate along the system, improving the yield.

Regarding the plasma separation in the HCTHPS devices, it relies on the creation of a CFL at the corner of each CEA. As shown at Figure 24b, RBCs move toward the central axis of the channels, when blood moves from a narrow constriction into a larger expansion, leading to the formation of a CFL [56].

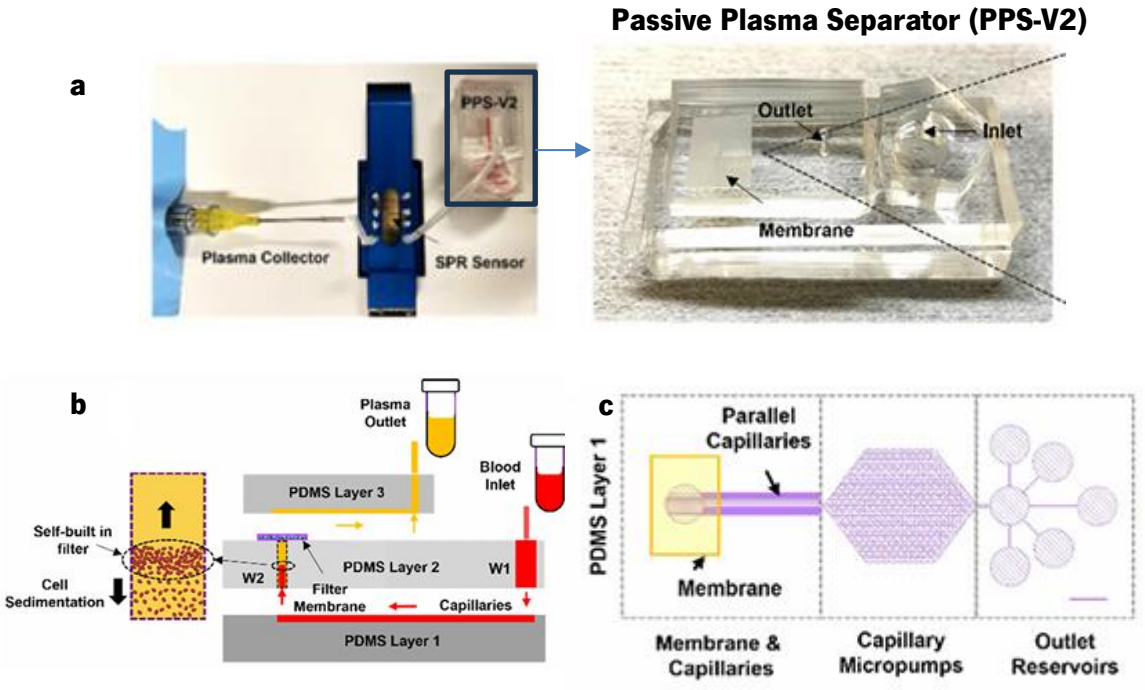



**Figure 23:** Operational principles of PPS-V2 system with SPR biosensor: (a) The PPS-V2 device assembled with membrane; (b) Schematic of the side view, exhibiting three PDMS layers and a membrane. The blood flows by capillary channels; (c) Top view of layer 3 design: capillaries, a capillary micropump and outlet reservoirs. Adapted and edited from [55].

This effect depends on the hematocrit content of the blood, the size and geometry of the CEA and the flow rate employed during operation. In this study, three versions were designed with different lengths of the side channel and with uniform plasma extraction rates, HCTHPS1, HCTHPS0.5 and HCTHPS0.25, being the last number the extraction rate per side channel. Using computational fluid dynamics (CFD) simulations, the team optimized flow rates to achieve the best balance between plasma purity and yield. Additionally, Abouali *et al.* tested the new devices using whole blood (45% hematocrit level), at flow rates of 5,10, and 15 mL/h to evaluate CFL formation, purity and yield of the plasma extracted. The device HCTHPS0.25 achieved a purity of 64% and a yield of 10%, the HCTHPS0.5 had 47% of purity and 18% of yield and the HCTHPS1 achived purity of 18% and yield of 35%. The HCTHPS0.25 device produced the widest CFL compared to the other versions, supporting earlier studies, that increasing extraction yield tends to reduce plasma's purity (as seen in HCTHPS1 device). However, the HCTHPS0.5 adressed this issue, demonstrating a better CFL formation than HCTHPS1 and indicating a balance between yield and purity. Furthermore, the flow rate 15 mL/h was the ideal for whole blood. Among the devices, they chose the HCTHPS0.5 since it provides a better yield compared to HCTHPS0.25 and a better purtiy compared to HCTHPS1. Additional analysis of CFL area under varying conditions suggested that a flow rate of 15

mL/h using whole blood offered the best performance. Additionally, blood samples were supplemented with different lactate concentrations (0.5 mM or 10mM) to compare the plasma quality achieved through conventional centrifugation and the microfluidic HCTHPS0.5 device. The plasma obtained was evaluated through aptamer bead-based fluorescence biosensing and electrochemical aptamer-based biosensing. The results showed that the plasma extracted by the HCTHPS0.5 had the quality to conduct analysis, having a better performance compared to centrifugation by lysing the RBCs to a lesser degree.

To conclude, these new three devices proved to efficiently separate plasma from human whole blood samples, enabling their use in subsequent biomarker analysis [56].

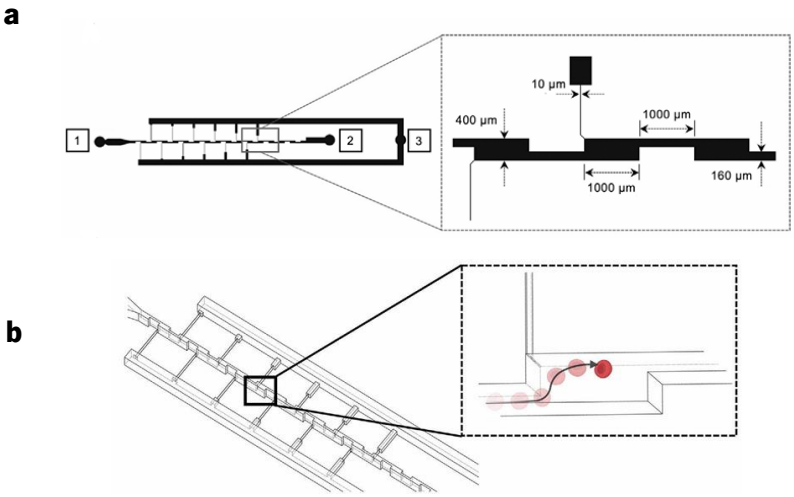



**Figure 24:** Plasma separation device through hemodynamic phenomena: (a) Schematic and dimensions of the system; (b) Illustration that demonstrates how cells flow through CEA and form the CFL [56].

### Deterministic lateral displacement

Darboui et *al.* developed a DLD microfluidic chip featuring crescent-shaped pillars for efficient plasma separation, inspired by the mechanism performed by fish gills (Figure 25a). The design was simulated using COMSOL software to optimize the geometry and the pillar shape, altering parameters such as spacing and diameter to achieve an accurate separation. In addition, the crescent array of pillars was fabricated using copper-assisted chemical etching (Cu-ACE, an economical alternative to precious metals) and was patterned on a PDMS layer. This approach included four components: a blood inlet containing a mixture of blood particles and plasma, two side reservoirs for collecting blood particles, and a plasma outlet for collecting the separated plasma.

The flow starts at a narrow channel, where filters were placed to stabilize the pressure in the wider section. At this section, the configuration of pillars consisted of five block of filters and were sited at progressively

wider gaps (h1-h4) (Figure 25b), forming arcing rows. Furthermore, the curvature of the columns resulted in the movement of the larger particles towards the chip walls and ultimately into the respective reservoirs. To prevent clogging or causing pressure slumps, each filter block started with the tiniest pillars (Q1) and was followed by progressively larger ones (Q2-Q4) (Figure 25b).

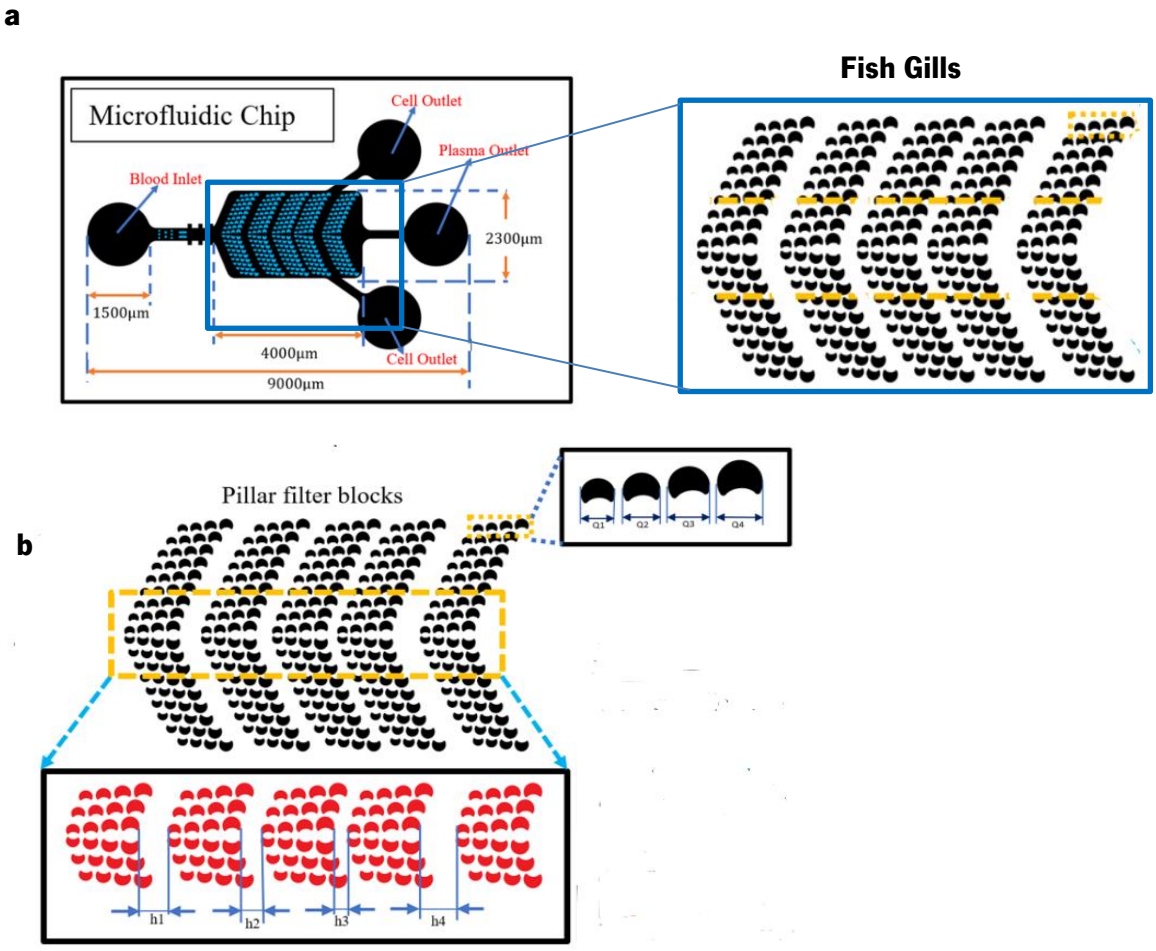



**Figure 25:** Microfluidic chip based on deterministic lateral displacement: (a) Dimensions and elements of the microfluidic chip; (b) Crescent-shaped filter and detailed schematic of its configurations. Five filters blocks positioned with gradually increasing gaps (h1-h4) and each filter block began with the smallest pillar size (Q1), followed by larger pillars (Q2-Q4). Adapted and edited from [46].

The variation in filter dimensions from one row to the next created a pore size gradient, which proved beneficial for separating particles of different diameters. Researchers concluded by simulations that tightening the space between successive blocks to about 50 µm while at the same time enlarging the pillars' diameter to 20 µm, improved the chip's effectiveness. Particles can lodge in the curved recesses

because the crescent profile itself increased the contact area between the filter walls and the blood flowing through them. Furthermore, two types of filter geometries were evaluated: spherical and crescent-shaped. The researchers found that when spherical filters were used, some blood particles entered the plasma reservoirs. In contrast, the crescent-shaped filters effectively prevented this issue.To evaluate the performance of the system, the team injected a diluted blood sample containing EDTA. Due to hydrodynamic forces, RBCs moved toward the walls of the channel because of their larger size and density, being expelled through the respective outlet. In contrast, plasma, with its lower density, gathered in the central area of the channel and was expelled through the central outlet. Finally, to assess the efficiency of the cell separation, the purity of the blood sample was calculated, being the blood cell count firstly measured through a hemocytometer. Thus, the plasma extracted had a purity of about 98% in 50 s, which indicated that the microfluidic chip is effective in separating blood cells from plasma and demonstrates the potential of Cu-ACE for the fabrication of microfluidic devices [46].

### 2.5.5 Hybrid methods

In the following selected published studies, the authors propose microfluidic devices that apply a combination of separation techniques.

#### Dielectrophoresis and filtration

An innovative approach was implemented by Dixon *et al.* through the introduction of a digital microfluidic (DMF) device for blood-plasma separation, which utilized a porous membrane integrated into a diagnostic platform (Figure 26). The major benefit of DMF devices is the integration of different applications on devices that use a generic architecture. This device was characterized by the manipulation of smaller sized droplets on an open surface, by the application of electric forces to an array of electrodes. In addition, this approach executed diagnostic tests and included a plasma separation membrane (SM), a transport membrane (TM) and a fluid-flow barrier. The SM allowed the red blood cells to be trapped in the larger pores of the membrane. On the other hand, the smaller pores allowed the filter plasma to flow. Moreover, the TM guaranted that the plasma was transported to the array of electrodes. Finally, the fluid-flow barrier prevented the sample from entering the membrane, being achieved by a wax plug (WP). The process to obtain plasma involved four steps and took around 4 min. Firstly, the device was connected to the Measles Rubella-Box (MR box), which is the digital microfluidic control system (Figure 26a). Its

primary function was to control droplet movement within the DMF by applying sine waves at a specific frequency. Subsequently, a droplet of extraction buffer was dispensed onto the array, along with a blood sample introduced into the SM. While the cells were retained by the SM, the plasma passed through to the TM (Figure 26b) and reached the WP, completing this step within 3 min. Then extraction buffer droplet flew through the TM, taking about 30 s (Figure 26c). The final step consisted in the separation between the membrane and the plasma (Figure 26d) containing the droplet, being the total duration of plasma separation close to 4 min. Additionally, the researchers compared the traditional method of centrifugation with the new one, in terms of cell-depletion, hemolysis and protein recovery. Regarding cell-depletion, no cells were seen in the resulted plasma by the DMF device, being these results comparable to conventional centrifugation and other microfluidic techniques, which removed 99.9991% and 89% to 99.9% of the cells, respectively. In addition, in terms of hemolysis, researchers concluded that the plasma produced by this new technique was non-hemolyzed. The third metric, protein recovery, showed that albumin recovery in centrifuge and DMF-generated plasma was similar, indicating that there was little depletion of protein using this system. The team selected specific filter materials with low non-specific protein binding, since filter-techniques had lower success than centrifugation at this metric due to the adsorption of proteins. This level of performance was similar to microfluidic filtration methods, which have shown protein recovery results from 63-100% compared to centrifuged samples. After the extraction of cell-free plasma, the researchers explored the possibility of coupling the DMF with a multi-step assay for diagnosis, quantifying the rubella virus (RV) IgG. The limit of detection of the device was demonstrated to be 1.9 IU/mL, with a limit of quantification of 3.6 IU/mL, being both limits under the diagnostic threshold defined by WHO (10 IU/mL). In previous versions the blood samples had to be prepared off-chip (samples were diluted and measured off-chip), contrary to this new approach that processes everything on-chip (integrated ELISA for RV IgG). In general, the DMF approach yields plasma comparable to that of the centrifugation [57].

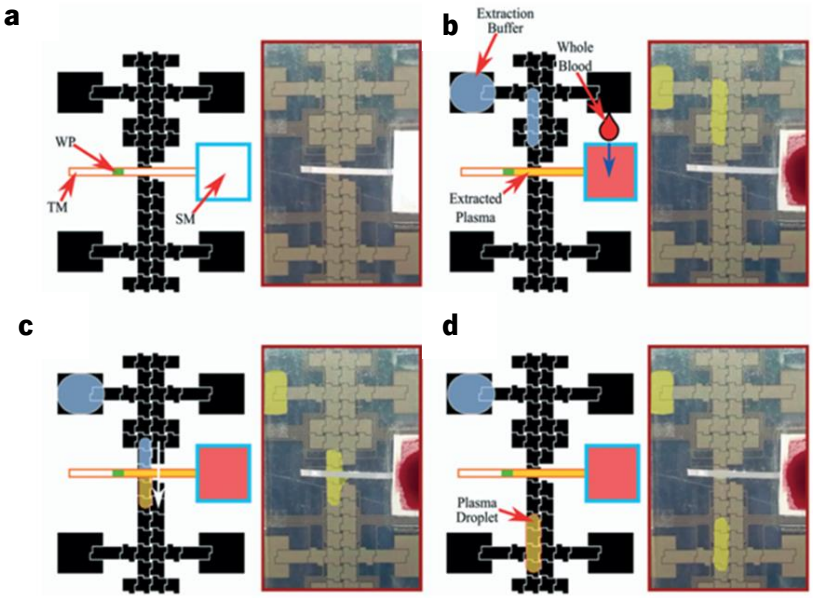



**Figure 26:** DMF blood-plasma separation: (a) Connection to the system unit; (b) Whole blood is loaded on the SM, where RBCs are trapped. Plasma flows to the electrode array, passing through the TM. Then the buffer is added to help collection; (c) Buffer moves across the membrane, pulling plasma with it into a droplet; (d) Plasma is inside the droplet and can be tested [57].

### Sedimentation and dielectrophoresis

Bakhtiaridoost *et al.* developed a microfluidic device that combines gravitational sedimentation with dielectrophoresis (Figure 27a, left side) to enhance the purity of the separated plasma, reduce processing time, and overcome the issue of air locking. This last obstacle resulted from the attempt of using a trench-based structure to accelerate the gravitational sedimentation of blood cells to separate plasma from whole blood. With air inside the trench, the blood cells do not enter the trench, following the path to the outlet above it. Researchers tried to overcome these limitations, however the approaches executed were time-consuming and damaged the blood cells. Therefore, the team conducted a microfluidic system to face the challenges mentioned previously. The system comprised an inlet, an outlet (for separated plasma), a cylindrical separation trench, and electrodes placed on the upper surface of the microchannel to generate negative dielectrophoretic force (Figure 27b). Regarding the microfluidic chip operation, a drop of blood was firstly introduced into the inlet using a syringe pump, pushing the air inside the microchannels out while the blood was entering the system. In addition, to overcome the trench's limitation, a layer of melt-blown polypropylene (MBPP) was used to cover the bottom of the trench, allowing the air to escape from the trench and preventing the blood from leaking out of the system. Consequently, by using this solution, the air exited faster through the trench than through the outlet, making the blood drawn into the trench.

The electrodes on top of the microchannel applied a non-uniform electrical field, creating a nDEP force. Consequently, the blood cells were repelled to the trench. Inside it, gravity acted on them. While blood cells were denser and sink to the bottom, the plasma was less dense and stayed on top, flowing then into the outlet channel. In practical terms, a drop of blood with 10 µL of undiluted blood was injected and it took less than 4 min to obtain 2.2 µL of plasma, without losing proteins. Furthermore, blood samples with different hematocrits (15-65%) were tested with applied voltages 0-20 Vpp. By using an optimized dielectrophoresis force, with an applied voltage of 20 Vpp, a plasma purity of 99.98%±0.02% was achieved, as determined by hemocytometry, surpassing the results reported *in prior* studies. The total protein obtained through the new device was also tested, 47.045 mg/ml, being considered similar to the results obtained through centrifugation. The suggested device is asimple and cost-effective tool for analysing different blood parameters due to its effectiveness in terms of separation speed, plasma quality, and yield, as well as its compatibility with downstream detection devices. [45].

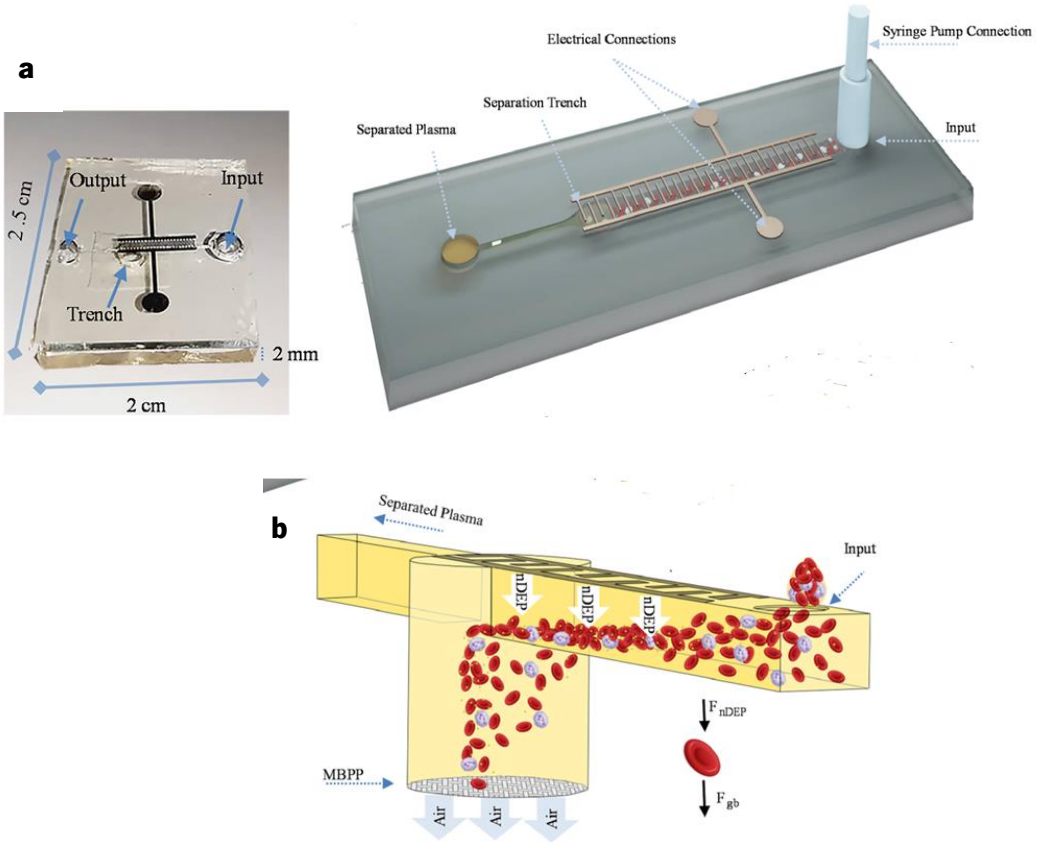



**Figure 27:** Microfluidic device to extract plasma from undiluted whole blood by gravitational sedimentation: (a) Left: prototype and right: schematic of the microsystem; (b) Working principle of the device- through nDEP force, cells flow to the bottom of the channel and are guided into the separation trench. Here gravity ($\boldsymbol{F_{gb}}$) acts on cells. The trench is sealed with MBPP layer, while plasma flows on top. Adapted and edited from [45].

CHAPTER 3

# 3. MATERIALS AND METHODOLOGIES

This chapter describes the materials used and the experimental procedure conducted to optimize the microfluidic chip to obtain plasma from whole blood samples. It details the devices and components, along with the reagents and their preparation before the experimental trials. Additionally, this section includes the step-by-step reasoning that was followed for evaluating and improving the chip's performance, guaranteeing its effectiveness for PoC diagnostics.

## 3.1 Materials

### 3.1.1 Devices and Components

Plasma generation chip Fluidic 168, and all necessary accessories *e.g.* male mini Luer plug, single reservoir 200 µL with mini Luer cap and mini Luer-to-Luer adapter, were obtained from *Microfluidic ChipShop.* Syringes with Luer interface were acquired from *BBraun.*

### 3.1.2 Reagents

Phosphate Buffered Saline tablets (PBS, 0.01 M phosphate buffer, 0.0027 M potassium chloride and 0.137M sodium chloride, pH 7.4, at 25°C, cat no. P4417) and ethylenediaminetetraacetic acid (EDTA, Anhydrous, cat no. EDS-100G), potassium hydroxide (KOH) and potassium chloride (KCl) were obtained from *Sigma-Aldrich.* Double distilled water ($ddH_2O$) was obtained using a double-pass distiller in the laboratory.

#### Preparation of Standard Solutions

A PBS solution was prepared by dissolving two tablets in 400 mL of $ddH_2O$, with each tablet formulated for 200 mL of water. The solution was stirred at RT using a magnetic stirrer until complete dissolution was achieved.

Another standard solution prepared was a 10%(w/v) EDTA anticoagulant. To obtain 50 mL of this solution with the previous concentration, 5 g of EDTA was dissolved in 50 mL of PBS and mixed by means of a magnetic stirrer. Additionally, since EDTA is not soluble in water at neutral or low pH, it was necessary to

adjust the pH to a range between 8.0 and 8.5 to ensure complete dissolution. The procedure began with the calibration of the pH meter using standard buffer solutions of pH 10, pH 7, and pH 4 to guarantee accurate pH measurements. Due to the initially low pH, a basic KOH solution was gradually added to raise the pH to the desired range. This solution was prepared in advance by dissolving the required mass of KOH, with a formula weight of 56.11 g/mol, in 100 mL of $ddH_2O$ water to achieve a concentration of 5 M. Once the EDTA had fully dissolved, the pH was carefully adjusted to 7.4 using an acidic KCl solution. This stepwise approach ensured complete solubilization of the EDTA and precise pH control, making the solution suitable for use with biological samples such as blood.

### 3.1.3 Biological samples

Capillary whole blood samples obtained via finger-prick were collected from healthy volunteers after obtaining informed consent.

**Capillary whole blood sample preparation**

Prior to evaluating the performance of the microfluidic chip for plasma extraction using undiluted capillary whole blood samples, the following protocol was followed. The process began with the careful unpacking of the chip and verification that all components were securely in place. According to the design specifications, the reservoir and male plugs were correctly fitted into their respective ports.
Next, 100 µL of the stock EDTA solution in PBS were pipetted into an eppendorf tube. From this, 10 µL were transferred to a separate eppendorf tube for later use. For blood collection, the fingertip was first sterilized with ethyl alcohol, and a lancet was used to obtain a drop of blood. This blood drop was then added to the eppendorf tube containing 10 µL of 10% (w/v) EDTA solution, and the total volume was adjusted to 250 µL in accordance with standard anticoagulation protocols. To ensure thorough mixing of the blood and anticoagulant, the tube was shaken gently to achieve a homogeneous solution.

## 3.2 Fluidic 168: specifications and experimental approach

The objective of this experiment was to optimize and validate the performance of a microfluidic chip designed to separate plasma from whole blood. The motivation behind this work lied in the development of an integrated all-in-one solution, with blood sample processing and molecular analysis directly at the PoC, thereby eliminating the need for preliminary sample processing in conventional laboratory settings. For this purpose, the plasma generation chip Fluidic 168, included in the microfluidic chip format group,

was selected due to its promising features. The device is made of a thermoplastic polymer named topas, designed for *in-situ* blood sample processing.It features four membranes, each with a diameter of 10 mm, enabling multiplexed separation and individual plasma extraction from four distinct whole blood samples. In addition, this chip was designed to separate whole blood from plasma using passive methods, namely capillary force and membrane filtration. Thus, the system followed the requirements for PoC applications such portability and minimally human intervention. Figure 28 presents a schematic representation of the chip Fluidic 168.



**Figure 28:** Schematic representation of the chip Fluidic 168 [58].

Theoretically, the process, schematically illustrated in Figure 29, begins with the introduction of blood sample through a single reservoir equipped with a mini Luer cap, which is placed at the Luer interface (1). Then, the blood sample flow through the support channel (2) toward the separation membrane (3), where the critical process of blood-plasma separation takes place. Once separated, the resultant plasma is collected in the plasma collection channel (4) located beneath the separation membrane. Furthermore, to ensure smooth operation and efficient filtration, a ventilation channel (5) helps balance the pressure during the separation process, being located below the membrane. The second interface (6), connects the collection channel to the external environment, enabling the application of vacuum to enhance filtration efficiency. Additionally, the third interface (7) plays a crucial role when blood elements clog the membrane pores. This interface can be opened to release the vacuum and restore functionality; however, it remains closed during sample loading to maintain system integrity [59].




**Figure 29:** Close-of photograph of the plasma generation chip Fluidic 168 elements [60]. Edited with Canva.

Although the chip Fluidic 168 was designed to perform plasma separation passively, as mentioned previously, practical implementation revealed some difficulties. The experimental workflow began with native undiluted whole blood, with the aim of assessing whether the system's intrinsic capillary forces, combined with the viscosity and other rheological properties of undiluted whole blood, would be sufficient to achieve consistent and efficient plasma separation. However, several obstacles were identified leading to low plasma separation. Consequently, plasma separation was hybridized, combining the passive techniques mentioned previously with active methods, including syringe- and pipette-driven suction, manual manipulation of the reservoir lid and insertion/removal of the male mini Luer plug. Each of the decisions was based on logical reasoning and followed a workflow, which was translated into a decision tree to help guide a methodical optimization pathway. This tree summarizes the choices made, formulated as binary (yes/no) questions. The diagrams illustrates the reasoning pathway adopted during the experimental procedure will be presented in subsection 3.2.1.

Although plasma was successfully obtained in the initial trials, persistent challenges remained and the results were inconsistent. As a result, the chip was further evaluated using blood samples prepared at different dilution levels, while active methods continued to be employed and adapted, until the most effective plasma separation method and optimal dilution level were identified.

### 3.2.1 Microfluidic optimization procedure: methodology adopted

As mentioned before, to optimize the microfluidic chip procedure, several series of experimental trials were conducted. Given the multiplex configuration with four membranes, each membrane was allocated for a single trial. The initial trials used undiluted capillary blood under varying conditions. Before detailing each one of the undiluted samples, Table 2 summarizes the key parameters explored in each

case, including sample composition, the use of capillary and/or mechanical forces and the operational mode of the chip: active, passive or hybride.

**Table 2:** Forces and operational mode applied in initial trials-undiluted capillary blood sample- -to optimize the microfluidic chip.

| Method | Sample | Capillarity and Filtration membrane | Mechanical force | Operational mode |
|---|---|---|---|---|
| **1** | **100 µL undiluted capillary whole blood** | yes | yes | Hybrid |
| **2** | **200 µL undiluted capillary whole blood** | yes | yes | Hybrid |

**First method tested: pressure equalization and vacuum application**

In this approach, 100 µL of undiluted capillary whole blood from the 250 µL tube containing the anticoagulant collected previously was loaded in the microfluidic chip inlet. The third interface (7 in Figure 29) was then opened to ensure pressure equalization through the membrane. The goal was to eliminate positive pressure generated during blood loading. After, a syringe was connected to the second interface to generate a negative pressure across the separation membrane. By pulling the plunger, the objective was to create vacuum, allowing plasma separation and driving blood through the membrane into the collection channel. Figure 30 presents a diagram of this procedure.

**Second method tested: pre-run with PBS and outlet suction via pipette**

In the second attempt, a pre-run was performed using 200 µL of PBS containing 1.6 mg/mL of EDTA to moisten the channels and membrane. Additionally, 200 µL of undiluted capillary whole blood was introduced into the inlet by mixing 10 µL of 10% (w/v) EDTA with 240 µL of undiluted whole blood, following the protocol described in Subsection 3.1.3. The only step executed differently was the use of a diabetic lancet to prick the finger, instead of a standard lancet. During this trial, gentle suction was applied at the outlet by setting the pipette to 20 µL. This controlled suction aimed to promote a stable flow from the membrane to the outlet through the application of negative pressure corresponding to a 20 µL aspiration, without imposing excessive mechanical stress. This procedure is shown at Figure 31.

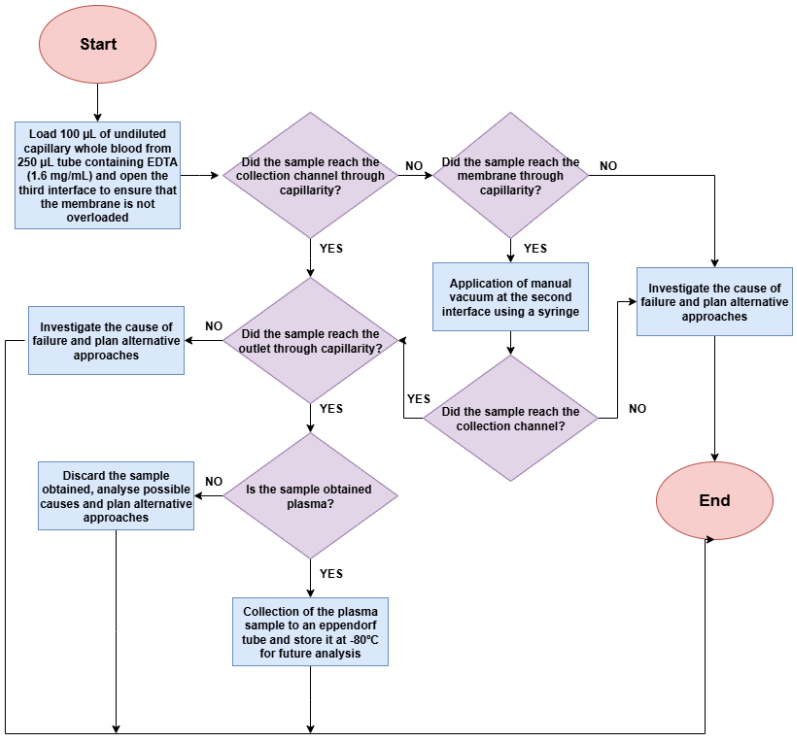



**Figure 30:** Decision digrama followed in the first attempt-methodology.

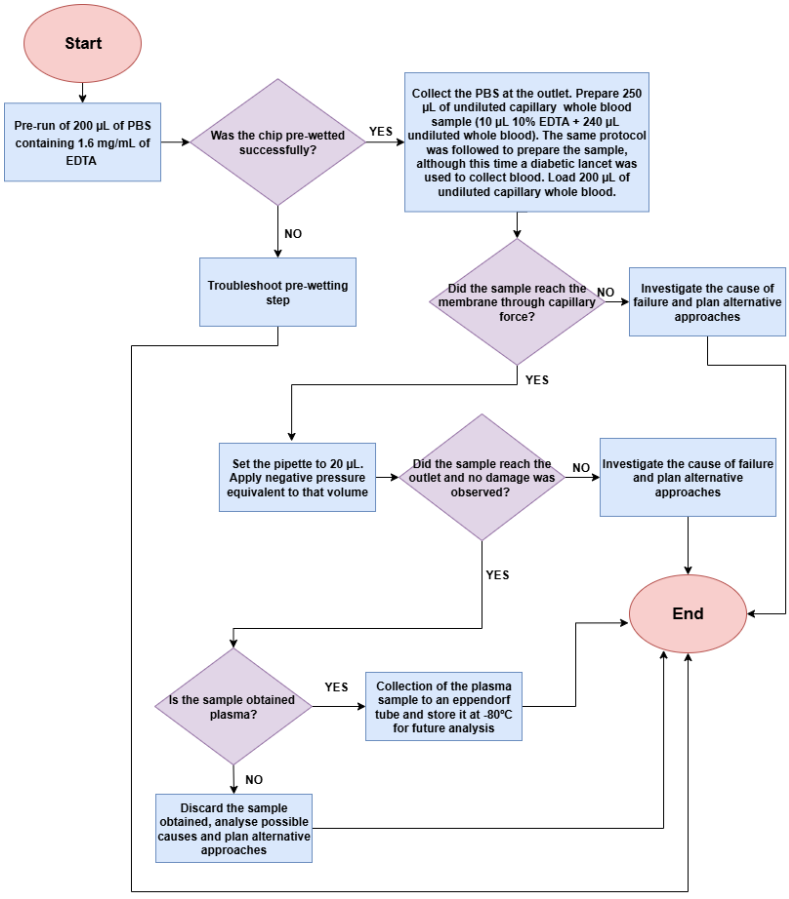



**Figure 31:** Decision digrama followed in the second attempt-methodology.

Despite the successful extraction of plasma without prior dilution, it was subsequently decided, following these trials, to assess samples across different dilution levels.This is important to improve efficiency and yield, to reduce the risk of hemolysis and clogging, and to ensure reproducibility. Therefore, the best trade-off between plasma quality, volume and chip performance can be found.

Initially, it was necessary to assess whether the EDTA anticoagulant caused hemolysis. The following paragraph outlines the methodology employed for this evaluation. To evaluate the impact of EDTA on the blood sample, a stock solution of 100 µL of 10%(w/v) EDTA in PBS (solution A) was prepared. Then, 10 µL of this stock solution was transferred to an eppendorf tube. Following the previously described finger-prick protocol, 240 µL of whole blood was collected into the tube, resulting in solution B.

Additionally, an EDTA solution with a concentration of 1.6 mg/mL in PBS and a total volume of 150 mL was prepared by diluting the stock solution, which had a concentration of 100 mg/mL, according to the following equation:

$$C1 \times V1 = C2 \times V2$$

where $C1$ represents the concentration of the stock solution (100 mg/mL), $V1$ is the volume of the stock solution to be calculated, and $C2$ (1.6 mg/mL) and $V2$ (150 mL) are the desired concentration and final volume of the diluted solution, respectively. To prepare 150 mL of EDTA solution in PBS at 1.6 mg/mL, 2.4 mL of the stock solution (100 mg/mL) was diluted in 147.6 mL of PBS (solution C).

The next steps involved preparing two eppendorf tubes, each with a total volume of 40 µL. The undiluted tube contained 20 µL of solution A and 20 µL of solution B, while the diluted tube included 20 µL of solution B and 20 µL of solution C. Both tubes were then centrifuged at 2700 rpm for 10 min. The results indicated that EDTA did not cause hemolysis.

### Trials with diluted capillary whole blood

In these trials, as described in the early tests, a pre-run with 100 µL of EDTA in PBS at a concentration of 1.6 mg/mL was executed before the loading of the blood samples. This step was consistently applied throughout the procedure to evaluate each sample: undiluted, 1:2 diluted, and 1:4 diluted whole blood samples. The sample preparation is listed at Table 3.

Plasma extraction was performed using only capillary action or, in some cases, with a combination of mechanical force. Mechanical force involved either opening and closing the reservoir lid or gently repeatedly pressing it with the thumb to enhance sample flow. In addition, this step was also executed

by inserting and removing the male mini Luer plug from the lid. Table 4 presents the forces applied during each approach and the operational mode of the microfluidic device.

**Table 3:** Samples along with the corresponding reagents and volumes used for preparing each solution to evaluate and optimize the plasma extraction microfluidic chip.

| **Samples** | **Biological Sample Preparation** |
|---|---|
| **Whole Blood (undiluted)** | 180 μL EDTA anticoagulant whole blood + 20 μL EDTA in PBS |
| **Whole Blood (1:2 dilution)** | 100 μL EDTA anticoagulant whole blood + 100 μL EDTA in PBS |
| **Whole Blood (1:4 dilution)** | 40 μL EDTA anticoagulant whole blood + 160 μL EDTA in PBS |

**Table 4:** Forces and operational mode applied in whole blood samples with different dilution levels.

| **Method** | **Sample** | **Capillarity/ Filtration membrane** | **Mechanical Force** | **Operational mode** |
|---|---|---|---|---|
| **3** | **200 μL whole blood (undiluted)** | yes | no | Passive |
| **4** | **200 μL whole blood (1:2 dilution)** | yes | no | Passive |
| **5** | **200 μL whole blood (1:4 dilution)** | yes | yes | Hybrid |
| **6** | **200 μL whole blood (1:4 dilution)** | yes | yes | Hybrid |

Figures 32, 33 and 34 present the decision diagrams, outlining the procedure followed for each diluted sample of whole blood.

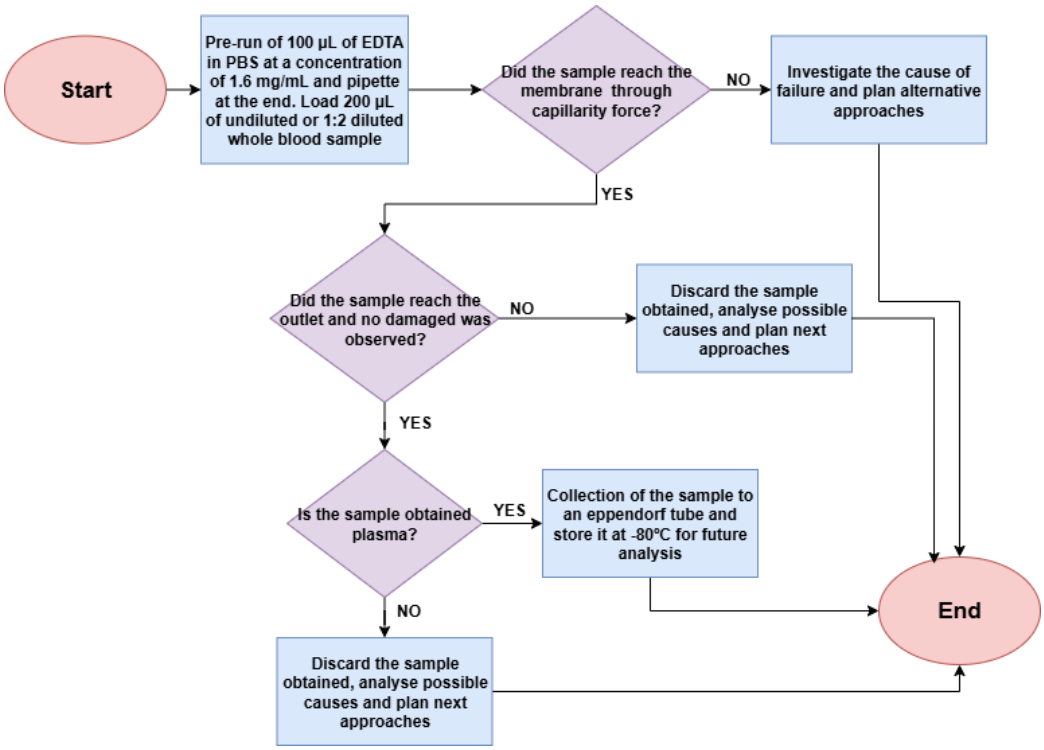



**Figure 32:** Decision digrama followed in the third and fourth attempt-methodology.

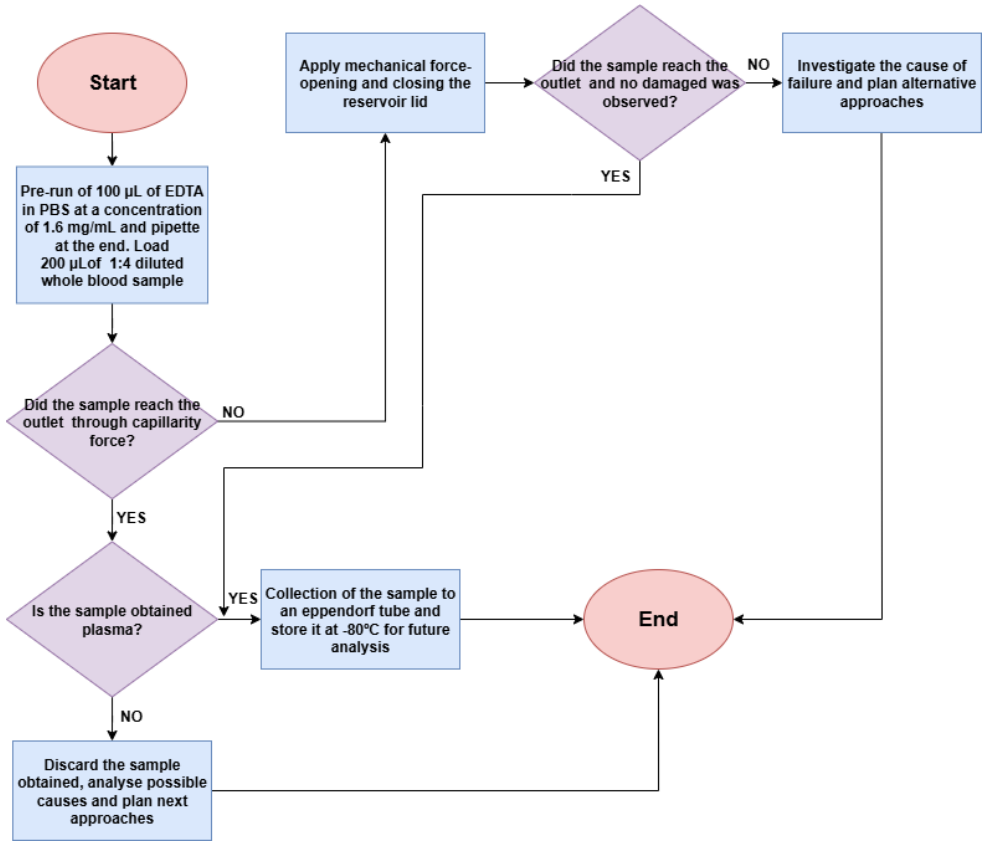



**Figure 33:** Decision digrama followed in fifth attempt-methodology.

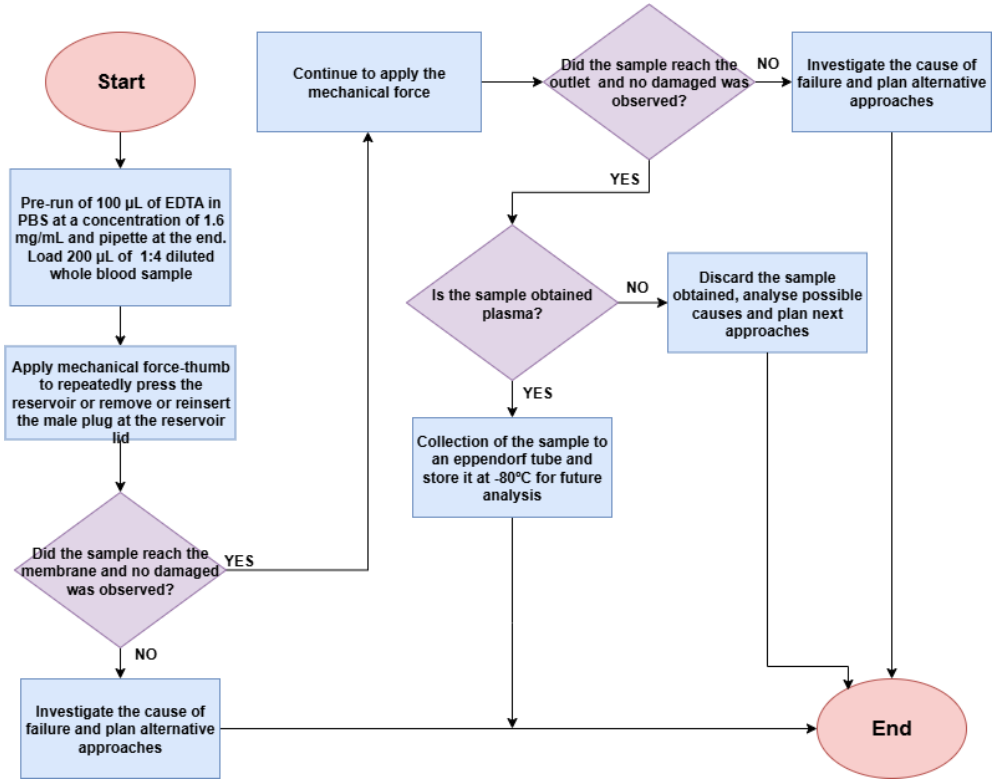



**Figure 34:** Decision digrama followed in the sixth attempt-methodology.

# 4. EXPERIMENTAL RESULTS AND DISCUSSION

This section reports the experimental results derived from the procedures outlined earlier and provides a critical assessment, situating the findings within the context of prior research..

## 4.1 Experimental results

The following table presents the results obtained in each trial, along with the respective forces applied to enhance blood-plasma separation at the microfluidic chip. The discussion of the results will be present in the next subsection.

**Table 5:** Results achieved in each trial with the respective forces and operational mode.

| Method | Sample | Forces applied | Operational mode | Results |
|---|---|---|---|---|
| **1** | **100 µL undiluted capillary whole blood** | Mechanical force: open the 3rd interface and apply vacuum at the 2nd interface using a syringe | Hybrid | Membrane rupture |
| **2** | **200 µL undiluted capillary whole blood** | Mechanical force: gentle outlet suction, pipette 20 µL at a time | Hybrid | 30 µL of plasma recovered |
| **3** | **200 µL undiluted capillary whole blood** | Capillarity force | Passive | Membrane clogged |
| **4** | **200 µL whole blood (1:2 dilution)** | Capillarity force | Passive | Membrane clogged |
| **5** | **200 µL whole blood (1:4 dilution)** | Capillarity and mechanical force- open and close the reservoir lid | Hybrid | Capillarity force: extract a small amount of plasma<br>Mechanical force: opening reservoir caused hemolysis |
| **6** | **200 µL whole blood (1:4 dilution)** | Mechanical force: thumb to gently and repeatedly press the reservoir or remove/insert mini Luer plug at the reservoir | Hybrid | Plasma recovered |

## 4.2 Discussion of the experimental results

### 4.2.1 First method tested: pressure equalization and vacuum application

In this attempt, the third interface was opened to allow pressure equalization, being connected to the ventilation channel below the membrane. Leaving it open during vacuum application through the second interface created a pathway for air to enter the system, while the air was simultaneously drawn by the syringe. Therefore, below the membrane was created a turbulent flow, causing instability to the membrane, which is sensitive to pressure variations. This resulted in deformation of the membrane, followed by its rupture This outcome suggests the importance of keeping the interfaces properly closed for the structural integrity of the membrane, enhancing the necessity for more controlled pressure to avoid damage.

### 4.2.2 Second method tested: pre-run with PBS and outlet suction via pipette

In the second approach, the controlled suction applied at the outlet by pipetting, helped the fluid to flow from the membrane to the outlet, which prevented undue pressure from damaging the membrane or interfering with blood flow. No membrane damage was observed throughout the process, indicating that the suction applied was appropriate.

At the conclusion of the procedure, an average of approximately 30 µL of plasma was recovered from 200 µL of capillary whole blood. This outcome demonstrates the system's capability to effectively separate plasma without compromising membrane or chip integrity. The recovered plasma was stored at minus 80°C for future analysis and preservation, ensuring viability for subsequent biomarker quantification. These results suggest that with consistent control of pressure, the microfluidic system has strong potential for efficient plasma extraction and diagnostic applications.

### 4.2.3 Trials with diluted capillary whole blood

During the loading of samples into the microfluidic chip in the third, fourth and fifth trials, several challenges related to blood sample handling were observed. Processing both undiluted and 1:2 diluted whole blood samples using the capillary method led to membrane clogging. This problem likely resulted from insufficient dilution, which failed to sufficiently reduce the cellular content, leading to membrane

obstruction. Red blood cells were a primary factor contributing to the blockage, underscoring the necessity of optimizing dilution to enable smooth flow through the microfluidic channels.

In the fifth trial with 1:4 diluted whole blood sample, both capillary action and mechanical force were employed. Capillary action was first used to extract a small volume of plasma. However, when the reservoir lid was opened and closed, hemolysis occurred. This was likely caused by the pressure applied during mechanical manipulation or the formation and agitation of air bubbles within the system. Hemolysis compromises the integrity of the plasma sample by releasing cellular contents, which can adversely impact subsequent analyses.

In the sixth trial, a new method was evaluated, involving the use of the thumb (Figure 35) to gently and repeatedly press the reservoir, thereby facilitating sample flow.

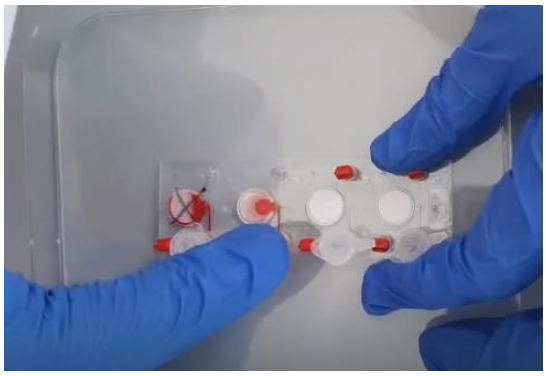


**Figure 35:** Photograph showing the application of mechanical force using the thumb to load the sample.

Using this technique, the liquid was successfully transferred from the channel to the membrane, increasing pressure and promoting plasma movement. Additionally, the male plug at the reservoir lid was also used to execute the same function by alternating between reinserting and removing it as the plasma reached the outlet. Figure 36 illustrates, as an example, the steps taken to evaluate the sixth trial. The "video" shown in the images below demonstrates only the example of the thumb pressure being applied. This attempt of applying pressure to the reservoir demonstrated better pressure control and facilitated the extraction of plasma. Figure 37 illustrates the plasma solution obtained from the sixth trial (yellower), compared to water (clearer). It confirms that the chip successfully converted whole blood into plasma.

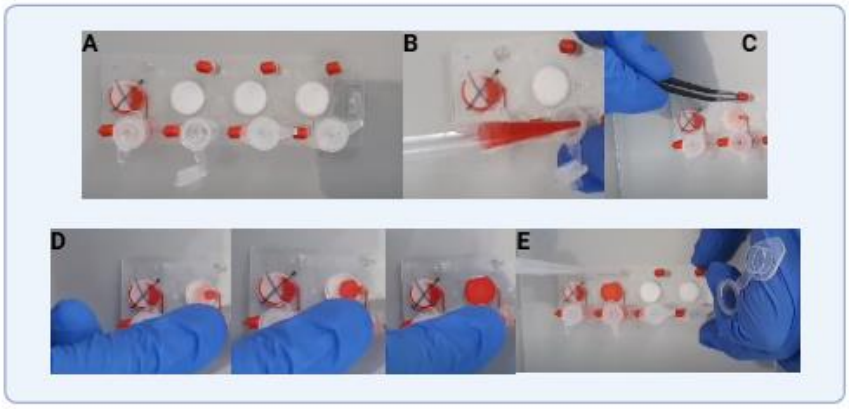



**Figure 36:** Photographs of the steps followed to load one of the samples: (a) Open the reservoir lid; (b) Inject the sample; (c) Remove the male mini Luer plug at the second interface; (d) Apply mechanical force with the finger to load the sample and (e) Collect the sample.

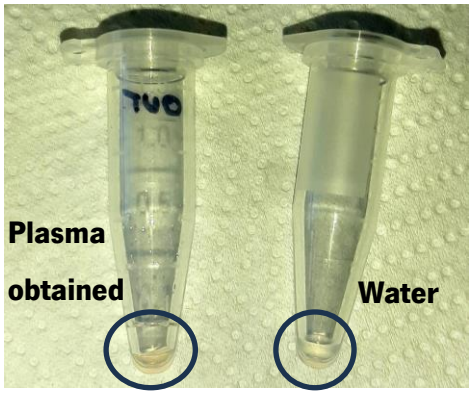



**Figure 37:** Plasma solution obtained by loading 1:4 diluted whole blood.

### 4.2.4 Assessing plasma separation performance

Among the various loading methods tested, the combination of a 1:4 diluted whole blood sample with manual pressure applied using the thumb or reinserting and removing the male plug at the reservoir lid, proved to be the most effective strategy for plasma extraction, as demonstrated in the final trial. This technique proved to prevent both clogging and hemolysis while allowing more controlled flow of the sample.

Overall, the successful plasma separation relies heavily on the proper dilution of blood samples and pressure regulation. While mechanical force can aid in plasma extraction, it must be applied with caution to prevent undesirable effects such as hemolysis, clogging and membrane rupture. These findings

underscore the necessity of optimizing both the dilution and force application parameters to achieve efficient plasma extraction while maintaining the integrity of the sample for subsequent analysis.

### 4.2.5 Comparison of the Fluidic 168 chip performance with the aforementioned literature

The Fluidic 168 was designed as a passive plasma separation device using capillary forces and membrane filtration, following the requirements of PoC applications, where portability and minimally human intervention are crucial. Although, during experimental trials, the device showed the need for mechanical forces in order to achieve plasma separation. Consequenlty, several approaches using mechanical force needed to be evaluated. All of this contributed to deviate from the initial goal of developing a purely passive device and introduced practical limitations for PoC applications. This device has become a hybrid system, thus combing the active forces (mechanical forces) with passive techniques such capillarity and membrane filtration. Furthermore, the diluted samples evaluated were all prepared off-chip, thus neither minimizing steps nor avoiding dependence on laboratory materials, as PoC applications demands.

As mentioned before, passive separation techniques of plasma usually achieve lower efficiency results, and need larger processing time and sample volumes to achieve satisfactory results. In addition, are simpler and cheaper. On the other hand, active methods obtain higher efficiency results, however their systems are complex and expensive. To compare this study with the aforementioned literature on both active and passive blood-plasma separation techniques, it is crucial to evaluate key metrics such yield, purity and extraction rate, as referred in section 2.4. All these parameters were not assessed in the present work and could be addressed in future studies. Nevertheless, some values were obtained during the trials. Solely in the third approach, 30 µL of plasma was extracted from 200 µL of undiluted whole blood, corresponding to a very low yield of 15%. This value is lower compared to the yield's results of the systems mentioned above. In addition, the need for manual application of pressure by thumb and male mini Luer plug (operator dependent) increase the risk of human errors and reduce reproducibility. Furthermore, this device does not integrate biomarker detection. On the other hand, benefits of the fluidic 168 are its simple design and easy fabrication. Furthermore, compared to active techniques, the fluidic 168 do not need acoustic, magnetic or dielectric forces, allowing its use for example in locals without electricity because the system only requires minimal handling. In addition, by concluding that pre-wetting and dilution might improve performance, the way for future fully passive solutions was enhanced.

Therefore, this work represents a crucial step toward the development of effective microfluidic systems for blood-plasma separation in PoC applications. In addition, it provides a solid foundation for future optimization, especially in refining the operational protocol, considering the microfluidic chip's sealed feature. This is described at section 5.2.

CHAPTER 5

# 5. CONCLUSION AND FUTURE PERSPECTIVES

This final section summarizes the main conclusions and findings from this project. The second part of this chapter examines possible future developments that can further expand and enhance the project.

## 5.1 Conclusions

This dissertation project proposed the optimization of a microfluidic chip for PoC blood-plasma extraction. This fluid plays a crucial role in clinical diagnostics, as it contains vital biomarkers essential for the early detection, monitoring, and prognosis of numerous diseases. In the field of PoC diagnostics, the ability to quickly and efficiently separate plasma from whole blood is essential, since PoC devices are designed to provide rapid, low-cost and decentralized testing. In addition, laboratory-based diagnostics nowadays involve invasive phlebotomy, complex and bulky equipments and time-consuming pre-processing steps, leading to delay diagnostics, especially in resource-limited settings or urgent scenarios. Therefore, addressing the goal of this project contributes to improve healthcare outcomes while reducing financial and logistical burdens.

Thus, to fulfill the main objective of the work, several methodologies were carried out to evaluate crucial parameters influencing the system's performance. The chip's capillarity, the application of mechanical force to complementary components and the effect of varying blood dilution levels (undiluted, 1:2 diluted and 1:4 diluted) were the parameters evaluated. Additionally, mechanical force was applied through different strategies, including opening the third interface while applying vacuum to the second interface using a syringe. Similar tests were conducted using a pipette. Moreover, the mechanical methods involved also the manual pressure to the reservoir lid with the thumb or the repeated insertion and remotion of the male mini Luer plug from the lid. After multiple trials, the most effective approach was found to be the use of 1:4 diluted whole blood sample loaded, in combination with one of the aforementioned manual pressure techniques. This method extracted plasma while avoiding hemolysis, clogging and without compromising the chip's integrity. However, the microfluidic chip did not perform as anticipated, ultimately yielding a system that depends on a combination of passive and active techniques. Furthermore, the most effective approach identified for plasma separation demanded manual operation,

which introduces variability and reduces the reproducibility of the method. Therefore, the protocol to extract plasma requires further improvements.

In the long term, this technology could be integrated into an all-in-one diagnostic platform, enabling rapid and accessible PoC testing by simultaneously pre-processing, analyzing, and quantifying blood biomarkers, thereby improving diagnostics at the PoC. Last but not least, this dissertation provided a comprehensive understanding of microfluidics and PoC diagnostics, significantly broadening my academic knowledge. As a direct outcome of this work, I co-authored the scientific article *Molecular Biomarkers for Timely and Prediction of Maternal-Fetal Health Risk*, published in the journal *Biomolecules* (doi: 0.3390/biom15030312). Furthermore, this research enabled my active participation in international conference (Living impact on fetal evolution), and key thematic workshops, including Workshop I: Regulations, Policy and Exploitation, Workshop II: Exploitation of R&D Results, enriching both my professional development and collaborative experience.

### 5.1.1 Objectives' Fulfilment

At the beginning of the project, a set of objectives was established to guide the optimization of a microfluidic chip for PoC blood-plasma extraction. This subsection outlines each objective and summarizes the extent to which it was achieved.

- **Objective 1:** Develop and optimize a protocol for rapid and efficient blood processing of finger-prick blood using a miniaturized microfluidic chip - Achieved.

A protocol was successfully developed that details the materials and reagents used, as well as various mechanical and capillary techniques employed to optimize the chip's usage and performance. All decisions were guided by logical reasoning and illustrated through diagrams. However, aspects of rapid and efficient blood processing could not be fully validated, because quantitative measurements such processing time and plasma yield were not evaluated. As such, further improvements in the protocol are required to obtain better results and enable chip's effective application in future analyses.

- **Objective 2:** Conduct preliminary tests to refine the plasma extraction process and assess potential hemolysis during sample loading - Achieved.

Preliminary tests played a crucial role in identifying key variables affecting chip performance, such as membrane behavior and the effects of different dilution levels. These insights formed the basis for evaluating the chip's overall performance. During the trials, hemolysis was detected under conditions characterized by abrupt or excessive pressure fluctuations, notably when the reservoir lid was opened and closed. This highlighted the pressure dynamics within the microfluidic system and emphasized the importance of maintaining controlled pressure to preserve plasma quality.

- **Objective 3:** Evaluate the efficiency of plasma extraction using the microfluidic chip- Achieved.

Among all the approaches evaluated in this project, the combination of 1:4 diluted whole blood with manual pressure applied by the thumb proved to be the most effective strategy. This technique enabled efficient plasma extraction while preventing membrane clogging and hemolysis, successfully achieving the main objective of optimizing the microfluidic chip for plasma extraction. Still, further improvements are necessary to fully realize its potential as a PoC device, rapid and efficient, as detailed below.

## 5.2 Future Perspectives

The successful optimization of the microfluidic chip procedures for extracting plasma from whole blood samples presented in this project marks a significant advancement in developing efficient PoC diagnostic tools. To fully realize this potential, key characteristics of PoC systems such as portability, sensitivity, speed, ease of use, and independence from complex equipment must be carefully addressed.

In this project, mechanical forces such as thumb pressure were used to ensure plasma extraction along with capillarity force and membrane separation. Future studies could explore automated or semi-automated actuation systems to improve consistency in pressure application, since manual thumb pressure introduces variability. Also, different users may apply varying levels of force, resulting in fluctuations in flow rate, pressure, and plasma yield. This user-dependent variability increases the risk of human error and reduces reproducibility. At the same time, the implementation of automated methods must be carefully considered to avoid compromising the portability essential for a PoC platform. Therefore, one example of improvement would be to hydrophilized the surface of the microfluidic chip. This treatment must be guaranteed by the supplier at the time of ordering. This consequently increases surface wettability, improves adhesion of aqueous solutions and reduces molecule adsorption, which improves device functionality. These changes should be tested with the aim of making plasma extraction

more efficient and faster, without the use of external forces and changes of the chip's structure. Another example of approach consists in the alteration of the chip's structure and operation. It consists in the construction of a vacuum reservoir connected at the blood sample inlet. This reservoir functions as an inverted syringe, containing a plunger. When whole blood is introduced into the reservoir, its weight exerts a downward force on the plunger, causing it to descend gradually. Consequently, the internal volume of the reservoir increases, generating a passive negative pressure at the inlet. As a result, the whole blood sample is sucked and drawn into the support's channel. The remaining components operate in accordance with the original system. By utilizing gravitational force to drive the plunger, this system works passively, generating controlled vacuum without external methods. In additional, mechanical stress on the separation membrane is avoided. Considering these reasons, this idea appears promising and well-suited for PoC applications, replacing the most effective approach of this project.

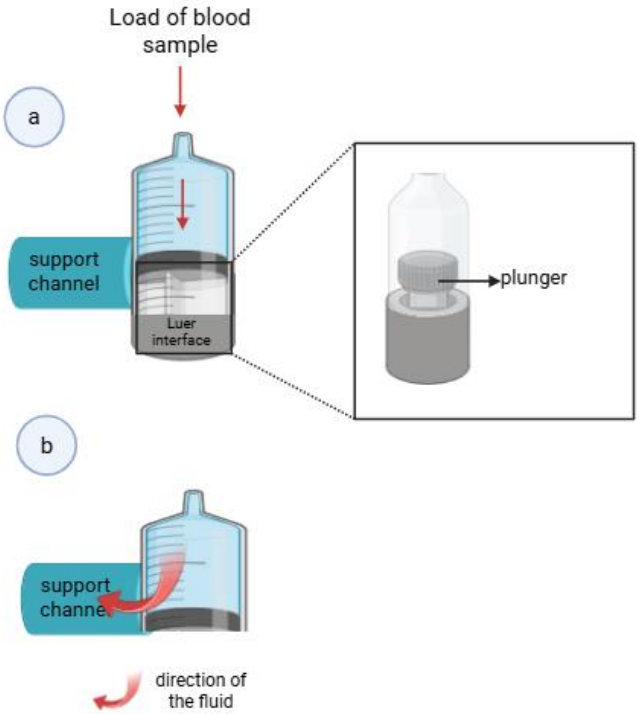



**Figure 38:** Power-free, weight-induced vacuum platform for plasma separation. Created with bioreneder. (a) Structure of the system; (b) Blood sample's weight creates a downward force, making the plunger descend. Vacuum is created, being the blood drawn into the support's channel.

In addition, to overcome the additional dilution steps, prior to the introduction of the sample into the vacuum reservoir, a preloaded reservoir with diluent should be used.

In the future, this microfluidic platform could be adapted to allow simultaneous on-chip processing, detection, and quantification of biomarkers related to, e.g. maternal-fetal health, at the PoC. To achieve this, future work should ensure that biomarkers do not interact adversely with the chip's membrane and are fully recovered at the outlet. Precise sample labelling and consistent, gentle handling are essential to minimize target molecule loss and ensure reliable results.

# 6. REFERENCES


[1] K. R. Baillargeon and C. R. Mace, "Microsampling tools for collecting, processing, and storing blood at the point-of-care," *Bioeng Transl Med*, vol. 8, no. 2, Mar. 2023, doi: 10.1002/btm2.10476.

[2] L. M. Rey Gomez, R. Hirani, A. Care, D. W. Inglis, and Y. Wang, "Emerging Microfluidic Devices for Sample Preparation of Undiluted Whole Blood to Enable the Detection of Biomarkers," *ACS Sens*, vol. 8, no. 4, pp. 1404–1421, Apr. 2023, doi: 10.1021/acssensors.2c02696.

[3] E. C. Rama and A. Costa-García, "Screen-printed Electrochemical Immunosensors for the Detection of Cancer and Cardiovascular Biomarkers," *Electroanalysis*, vol. 28, no. 8, pp. 1700–1715, Aug. 2016, doi: 10.1002/elan.201600126.

[4] S. Rosskopf *et al.*, "The pre-analytical processing of blood samples for detecting biomarkers on protein microarrays," *J Immunol Methods*, vol. 418, pp. 39–51, Mar. 2015, doi: 10.1016/j.jim.2015.01.009.

[5] E. Bakker *et al.*, "Biomarker Qualification at the European Medicines Agency: A Review of Biomarker Qualification Procedures From 2008 to 2020," *Clin Pharmacol Ther*, vol. 112, no. 1, pp. 69–80, Jul. 2022, doi: 10.1002/cpt.2554.

[6] P. S. S. 2, S. M. K. 3, S. P. K. 4, K. T. A. R. R. M. F. A. A. 8 Jisha U.*1, "A Review On Mastering Bioanalytical Sample Preparation Techniques: Achieving Accurate Analysis," *INTERNATIONAL JOURNAL OF PHARMACEUTICAL SCIENCES*, Aug. 2024.

[7] D. Basu and R. Kulkarni, "Overview of blood components and their preparation," *Indian J Anaesth*, vol. 58, no. 5, p. 529, 2014, doi: 10.4103/0019-5049.144647.

[8] S.-M. Yang, S. Lv, W. Zhang, and Y. Cui, "Microfluidic Point-of-Care (POC) Devices in Early Diagnosis: A Review of Opportunities and Challenges," *Sensors*, vol. 22, no. 4, p. 1620, Feb. 2022, doi: 10.3390/s22041620.

[9] S. T. Sanjay, M. Dou, J. Sun, and X. Li, "A paper/polymer hybrid microfluidic microplate for rapid quantitative detection of multiple disease biomarkers," *Sci Rep*, vol. 6, no. 1, p. 30474, Jul. 2016, doi: 10.1038/srep30474.

[10] H. Yuan, P.-Y. Chiu, and C.-F. Chen, "Paper-based analytical devices for point-of-care blood tests," *Biomicrofluidics*, vol. 15, no. 4, Jul. 2021, doi: 10.1063/5.0055601.

[11] P. Š. M. H. A. Š. M. D. D. L. P. D. T. V. J. B. L. V. K. H. N. T. H. L. M. P. B. Věra Křížková, *BLOOD and BLOOD COMPONENTS KAROLINUM u č e b n í t e x t y Unive r zit y K a r l o v y v*

*P r a z e Hematopoiesis, Selected Methods Used in Cytology, Histology, and Hematology*, First Edition. Prague: Charles University Karolinum Press, 2021.

[12] J. Lazarovits, Y. Y. Chen, E. A. Sykes, and W. C. W. Chan, "Nanoparticle–blood interactions: the implications on solid tumour targeting," *Chemical Communications*, vol. 51, no. 14, pp. 2756–2767, 2015, doi: 10.1039/C4CC07644C.

[13] H. Li, D. Han, M. A. Hegener, G. M. Pauletti, and A. J. Steckl, "Flow reproducibility of whole blood and other bodily fluids in simplified no reaction lateral flow assay devices," *Biomicrofluidics*, vol. 11, no. 2, Mar. 2017, doi: 10.1063/1.4979815.

[14] E. C. Lynch, *Peripheral Blood Smear*. 1990.

[15] Clinical and Laboratory Standard Institute, "PRE04 Handling, Transport, Processing, and Storage of Blood Specimens for Routine Laboratory Examinations."

[16] J. B. Vaught, "Blood Collection, Shipment, Processing, and Storage," *Cancer Epidemiology, Biomarkers & Prevention*, vol. 15, no. 9, pp. 1582–1584, Sep. 2006, doi: 10.1158/1055-9965.EPI-06-0630.

[17] My Hematology, "Blood Collection Tube (Vacutainer) Types." Accessed: Jan. 10, 2025. [Online]. Available: https://myhematology.com/lab-protocols/blood-collection-tube-types/

[18] Hindustan Syringes & Medical Devices Ltd, "Decoding the Colour Codes of Evacuated Blood Collection Tubes", Accessed: Jan. 10, 2025. [Online]. Available: https://hmdhealthcare.com/blog/decoding-the-colour-codes-of-evacuated-blood-collection-tubes/

[19] Express Lab, "Collection and Handling Tips." Accessed: Jan. 10, 2025. [Online]. Available: https://www.expresslabidaho.com/collection-tips/order-of-draw-3/

[20] Lexington Medical Center, "SPECIMEN COLLECTION, HANDLING, and TRANSPORT."

[21] World Health Organization, *WHO Guidelines on Drawing Blood Best Practices in Phlebotomy*. 2010.

[22] UK Biobank, "Blood Sample Collection, Processing and Transport," Apr. 15, 2011. Accessed: Jan. 20, 2025. [Online]. Available: https://biobank.ctsu.ox.ac.uk/crystal/crystal/docs/Bloodsample.pdf

[23] Ph. D. , D. J. D. B. M. D. D. J. E. M. T. (ASCP) S. S. S. D. I. S. M. A. , M. T. (ASCP), S. D. J. W. Ph. D. , M. B. A. J. D. W. M. T. (ASCP), C. Roger R. Calam, "Procedures for the Handling and Processing of Blood Specimens; Approved Guideline," 3rd ed., vol. 24, Pennsylvania, 2004.

[24] Edward-Elmhurst Health, "Blood Collection and Handling."

[25] M. Toner and D. Irimia, “Blood-on-a-Chip,” *Annu Rev Biomed Eng*, vol. 7, no. 1, pp. 77–103, Aug. 2005, doi: 10.1146/annurev.bioeng.7.011205.135108.

[26] K. Gandhi, N. Sharma, P. B. Gautam, R. Sharma, B. Mann, and V. Pandey, *Advanced Analytical Techniques in Dairy Chemistry*. New York, NY: Springer US, 2022. doi: 10.1007/978-1-0716-1940-7.

[27] R.Hinton and M.Dobrota, *Laboratory Techniques In Biochemistry And Molecular Biology*, vol. 6. Elsevier/North-Holland Biomedical Press.

[28] H. Kim, H. Park, D. R. Chung, T. Kim, E. Park, and M. Kang, “A self-pressure-driven blood plasma-separation device for point-of-care diagnostics,” *Talanta*, vol. 247, p. 123562, Sep. 2022, doi: 10.1016/j.talanta.2022.123562.

[29] W. Brakewood, K. Lee, L. Schneider, N. Lawandy, and A. Tripathi, “A capillary flow-driven microfluidic device for point-of-care blood plasma separation,” *Frontiers in Lab on a Chip Technologies*, vol. 1, Nov. 2022, doi: 10.3389/frlct.2022.1051552.

[30] M. Kersaudy-Kerhoas and E. Sollier, “Micro-scale blood plasma separation: from acoustophoresis to egg-beaters,” *Lab Chip*, vol. 13, no. 17, p. 3323, 2013, doi: 10.1039/c3lc50432h.

[31] H. Zhang *et al.*, “A circular gradient-width crossflow microfluidic platform for high-efficiency blood plasma separation,” *Sens Actuators B Chem*, vol. 354, p. 131180, Mar. 2022, doi: 10.1016/j.snb.2021.131180.

[32] M. Sonker, V. Sahore, and A. T. Woolley, “Recent advances in microfluidic sample preparation and separation techniques for molecular biomarker analysis: A critical review,” *Anal Chim Acta*, vol. 986, pp. 1–11, Sep. 2017, doi: 10.1016/j.aca.2017.07.043.

[33] B.-J. Lai, L.-T. Zhu, Z. Chen, B. Ouyang, and Z.-H. Luo, “Review on Blood Flow Dynamics in Lab-on-a-Chip Systems: An Engineering Perspective,” *Chem & Bio Engineering*, vol. 1, no. 1, pp. 26–43, Feb. 2024, doi: 10.1021/cbe.3c00014.

[34] R. García-Azuma, K. Werner, C. Revilla-Monsalve, O. Trinidad, N. F. Altamirano-Bustamante, and M. M. Altamirano-Bustamante, “Unveiling the state of the art: a systematic review and meta-analysis of paper-based microfluidic devices,” *Front Bioeng Biotechnol*, vol. 12, Aug. 2024, doi: 10.3389/fbioe.2024.1421831.

[35] F. Burgos-Flórez, A. Rodríguez, E. Cervera, M. De Ávila, M. Sanjuán, and P. J. Villalba, “Microfluidic Paper-Based Blood Plasma Separation Device as a Potential Tool for Timely Detection of Protein Biomarkers,” *Micromachines (Basel)*, vol. 13, no. 5, p. 706, Apr. 2022, doi: 10.3390/mi13050706.

[36] P. Pattanayak *et al.*, “Microfluidic chips: recent advances, critical strategies in design, applications and future perspectives,” *Microfluid Nanofluidics*, vol. 25, no. 12, p. 99, Dec. 2021, doi: 10.1007/s10404-021-02502-2.

[37] C. M. Miyazaki, E. Carthy, and D. J. Kinahan, “Biosensing on the Centrifugal Microfluidic Lab-on-a-Disc Platform,” *Processes*, vol. 8, no. 11, p. 1360, Oct. 2020, doi: 10.3390/pr8111360.

[38] Z. Du, J. Lin, B. Lin, and S. Yang, “Research advances in centrifugal microfluidics and its applications,” *Microchemical Journal*, vol. 213, p. 113589, Jun. 2025, doi: 10.1016/j.microc.2025.113589.

[39] S. A. Mateen and K. S. Bhole, “A review on microfluidic devices for separation of blood constituents,” *IOP Conf Ser Mater Sci Eng*, vol. 810, no. 1, p. 012024, Mar. 2020, doi: 10.1088/1757-899X/810/1/012024.

[40] A. Maurya, J. S. Murallidharan, A. Sharma, and A. Agarwal, “Microfluidics geometries involved in effective blood plasma separation,” *Microfluid Nanofluidics*, vol. 26, no. 10, p. 73, Oct. 2022, doi: 10.1007/s10404-022-02578-4.

[41] A. Shiriny and M. Bayareh, “On magnetophoretic separation of blood cells using Halbach array of magnets,” *Meccanica*, vol. 55, no. 10, pp. 1903–1916, Oct. 2020, doi: 10.1007/s11012-020-01225-y.

[42] K. Torres-Castro, K. Acuña-Umaña, L. Lesser-Rojas, and D. Reyes, “Microfluidic Blood Separation: Key Technologies and Critical Figures of Merit,” *Micromachines (Basel)*, vol. 14, no. 11, p. 2117, Nov. 2023, doi: 10.3390/mi14112117.

[43] A. Alazzam, B. Mathew, and S. Khashan, “Microfluidic Platforms for Bio-applications,” 2017, pp. 253–282. doi: 10.1007/978-3-319-32180-6_12.

[44] S. O. Catarino, R. O. Rodrigues, D. Pinho, J. M. Miranda, G. Minas, and R. Lima, “Blood Cells Separation and Sorting Techniques of Passive Microfluidic Devices: From Fabrication to Applications,” *Micromachines (Basel)*, vol. 10, no. 9, p. 593, Sep. 2019, doi: 10.3390/mi10090593.

[45] S. Bakhtiaridoost, H. Habibiyan, and H. Ghafoorifard, “A microfluidic device to separate high-quality plasma from undiluted whole blood sample using an enhanced gravitational sedimentation mechanism,” *Anal Chim Acta*, vol. 1239, p. 340641, Jan. 2023, doi: 10.1016/j.aca.2022.340641.

[46] M. Darboui, M. Fatehi, R. Zareifar, H. R. T. Tolgari, and H. E. Khoshmardan, "Multi-level DLD microfluidic chip for plasma separation: A novel approach using Cu-ACE," *Results Phys*, vol. 71, p. 108209, Apr. 2025, doi: 10.1016/j.rinp.2025.108209.

[47] D. Bento, C. S. Fernandes, J. M. Miranda, and R. Lima, "In vitro blood flow visualizations and cell-free layer (CFL) measurements in a microchannel network," *Exp Therm Fluid Sci*, vol. 109, p. 109847, Dec. 2019, doi: 10.1016/j.expthermflusci.2019.109847.

[48] H. Tanjaya *et al.*, "A review of Microfluidic blood separation techniques," *E3S Web of Conferences*, vol. 426, p. 01063, Sep. 2023, doi: 10.1051/e3sconf/202342601063.

[49] S. N. Ashrafizadeh, M. Zare, and M. Khatibi, "A comprehensive review of pinch flow fractionation in microfluidics: From principles to practical applications," *Chemical Engineering and Processing - Process Intensification*, vol. 208, p. 110087, Feb. 2025, doi: 10.1016/j.cep.2024.110087.

[50] S. Kwon, J. Oh, M. S. Lee, E. Um, J. Jeong, and J. H. Kang, "Enhanced Diamagnetic Repulsion of Blood Cells Enables Versatile Plasma Separation for Biomarker Analysis in Blood," *Small*, vol. 17, no. 23, Jun. 2021, doi: 10.1002/smll.202100797.

[51] L. Zeng *et al.*, "Power-free plasma separation based on negative magnetophoresis for rapid biochemical analysis," *Microsyst Nanoeng*, vol. 10, no. 1, p. 207, Dec. 2024, doi: 10.1038/s41378-024-00837-8.

[52] S. C. Liu, P. B. Yoo, N. Garg, A. P. Lee, and S. Rasheed, "A microfluidic device for blood plasma separation and fluorescence detection of biomarkers using acoustic microstreaming," *Sens Actuators A Phys*, vol. 317, p. 112482, Jan. 2021, doi: 10.1016/j.sna.2020.112482.

[53] Z. Ma *et al.*, "An acoustofluidic device for the automated separation of platelet-reduced plasma from whole blood," *Microsyst Nanoeng*, vol. 10, no. 1, p. 83, Jun. 2024, doi: 10.1038/s41378-024-00707-3.

[54] C.-C. Chen, P.-H. Lin, and C.-K. Chung, "Microfluidic chip for plasma separation from undiluted human whole blood samples using low voltage contactless dielectrophoresis and capillary force," *Lab Chip*, vol. 14, no. 12, p. 1996, 2014, doi: 10.1039/c4lc00196f.

[55] N. Debnath, L. S. Live, and M. Poudineh, "A microfluidic plasma separation device combined with a surface plasmon resonance biosensor for biomarker detection in whole blood," *Lab Chip*, vol. 23, no. 4, pp. 572–579, 2023, doi: 10.1039/D2LC00693F.

[56] H. Abouali, F. Keyvani, S. A. Hosseini, S. Srikant, and M. Poudineh, "Continuous High-Throughput Plasma Separation for Blood Biomarker Sensing Using a Hydrodynamic Microfluidic Device," *Adv Healthc Mater*, vol. 14, no. 9, Apr. 2025, doi: 10.1002/adhm.202404193.

[57] C. Dixon, J. Lamanna, and A. R. Wheeler, “Direct loading of blood for plasma separation and diagnostic assays on a digital microfluidic device,” *Lab Chip*, vol. 20, no. 10, pp. 1845–1855, 2020, doi: 10.1039/D0LC00302F.

[58] Microfluidic Chipshop, “Fluidic 168 Membrane Chips- Plasma Generation Chips.” Accessed: Nov. 20, 2024. [Online]. Available: https://www.microfluidic-chipshop.com/catalogue/microfluidic-chips/polymer-chips/membrane-chips/membrane-chips-fluidic-168/

[59] Microfluidic Chipshop, “Cell Culture and Membrane Chips.” Accessed: Nov. 20, 2024. [Online]. Available: https://www.microfluidic-chipshop.com/catalogue/microfluidic-chips/polymer-chips/membrane-chips/

[60] microfluidic ChipShop, “microfluidic ChipShop Lab-on-a-Chip Catalogue.” Accessed: Jun. 01, 2024. [Online]. Available: https://www.microfluidic-chipshop.com/wp-content/uploads/microfluidic-ChipShop_Lab-on-a-Chip-Catalogue_10_2023.pdf